Joint Two-Tier User Association and Resource Management for Integrated Satellite-Terrestrial Networks

Hung Nguyen-Kha, *Graduate Student Member, IEEE*, Vu Nguyen Ha, *Senior Member, IEEE*, Eva Lagunas, *Senior Member, IEEE*, Symeon Chatzinotas, *Fellow, IEEE*, and Joel Grotz, *Senior Member, IEEE*

***Abstract*— This paper investigates the uplink transmission of an integrated satellite-terrestrial network, wherein the low-earth-orbit (LEO) satellites provide backhaul services to isolated cellular base stations (BSs) for forwarding mobile user (UE) data to the core network. In this integrated system, the high mobility of LEO satellites (LEOSats) introduces significant challenges in managing radio resource allocation (RA), as well as the associations between UEs, BSs, and LEOSats for supporting users' demands efficiently, while also dynamically balancing the capacity of UE-BS access and BS-LEO backhaul links. Regarding these critical issues, the paper aims to jointly optimize the two-tier UE-BS and BS-LEOSat association, sub-channel assignment, bandwidth allocation, and power control to meet users' demands in the shortest transmission time. This optimization problem, however, falls into the category of mixed-integer non-convex programming, making it very challenging and requiring advanced solution techniques to find optimal solutions. To tackle this complex problem efficiently, we first develop an iterative centralized algorithm by utilizing convex approximation and compressed-sensing-based methods to deal with binary variables. Furthermore, for practical implementation and to offload computation from the central processing node, we propose a *Dec-Alg* that can be implemented in parallel at local controllers and achieve efficient solutions. Numerical results are also illustrated to strengthen the effectiveness of our proposed algorithms compared to traditional greedy and benchmark algorithms.**

***Index Terms*— LEO constellation, integrated satellite-terrestrial networks, resource allocation, user association.**

I. Introduction

RECENT years have witnessed a rapid development of terrestrial networks (TNs), marked by an increase in the number of connected devices, and the expansion of services and applications. This evolution necessitates the next-generation wireless communication networks be capable to meet the growth in cellular traffic demand and to satisfy various service requirements such as massive connectivity, seamless connectivity, and high reliability across global coverage [2], [3], [4], [5], [6]. In response to these pressing demands, TN infrastructure providers are compelled to deploy an increased number of BSs to enlarge network coverage and capacity. However, this solution poses considerable challenges, mainly due to the prohibitive costs associated with implementing backhaul links connecting these BSs to the core network [7]. It becomes more critical for the rural regions, suburban areas, mountainous terrains, and oceanic expanses due to the low economic efficiency [8]. To overcome these challenges, integrating satellites with cellular systems to establish integrated satellite-terrestrial networks (ISTNs) has been considered as a promising solution for future global connectivity [2], [9], [10], [11].

Previously, the satellite-based connection was considered a last resort for cellular backhaul due to bandwidth limitations and high costs; however, advancements in the satellite industry, particularly non-geostationary satellite constellations and ground segment innovations, have transformed satellite backhaul into a key solution, not only extending the mobile network coverage but also supporting high-quality broadband connectivity. Compared to geostationary (GEO) and medium-earth-orbit (MEO) systems, LEOSat constellations (including the very-low-earth-orbit) demonstrate additional benefits for certain applications when connecting the terrestrial BSs to the core network [12]. In particular, their lower altitude ensures lower latency in data transmission which is suitable for applications requiring near-real-time communication [13], [14]. In addition, the lower altitudes which are equivalent to the higher channel gains, also make LEOSats to be capable of supporting high data rate transmissions [13].

Despite the substantial advantages of global coverage, higher channel gain, and low transmission latency, the integration of LEOSats and TNs also poses significant challenges in dynamic network management. Specifically, the inherent high mobility of LEOSats requires novel dynamic association strategies to establish stable two-hop links between UEs, BSs, and LEOSats. In addition, the RA mechanism

Manuscript received 9 August 2023; revised 19 December 2023 and 3 June 2024; accepted 12 August 2024. Date of publication 23 August 2024; date of current version 13 November 2024. This research was funded in whole, or in part, by the Luxembourg National Research Fund (FNR) through the Project INtegrated Satellite—TeRrestrial Systems for Ubiquitous Beyond 5G CommunicaTions (INSTRUCT) under Grant IPBG19/14016225/INSTRUCT. An earlier version of this paper was presented at ICC Workshop 6GSatComNet'23 [DOI: 10.1109/ICCWorkshops57953.2023.10283736]. The associate editor coordinating the review of this article and approving it for publication was K. Xue. *(Corresponding author: Hung Nguyen-Kha.)*

Hung Nguyen-Kha, Vu Nguyen Ha, Eva Lagunas, and Symeon Chatzinotas are with the Interdisciplinary Centre for Security, Reliability and Trust (SnT), University of Luxembourg, 1855 Luxembourg, Luxembourg (e-mail: khahung.nguyen@uni.lu; vu-nguyen.ha@uni.lu; eva.lagunas@uni.lu; Symeon.Chatzinotas@uni.lu).

Joel Grotz is with SES, 6815 Betzdorf, Luxembourg (e-mail: Joel.Grotz@ses.com).

Color versions of one or more figures in this article are available at https://doi.org/10.1109/TWC.2024.3445266.

Digital Object Identifier 10.1109/TWC.2024.3445266

should be designed carefully to maintain user traffic demands while dynamically balancing the capacity of UE-BS access and BS-LEO backhaul links. The novel design should be well developed to ensure seamless handovers, manage power control, and mitigate cross-interference among all terrestrial access points [9], [10]. Hence, jointly optimizing the transmission and association strategies for LEO-based ISTNs has raised an important and challenging research topic.

A. Related Works

Recently, developing novel RA mechanisms for the ISTNs and user selection problems have received significant attention in research works [15], [16], [17], [18], [19], [20], [21], [22], [23], [24], [25]. Particularly, the authors in [15] studied the service pricing and user selection problem, wherein evolutionary game-based framework is proposed to solve the user-computation provider association problem under the computation requirement of users. In [16] a LEOSat is deployed to assist the TNs for cache offloading, wherein power allocation, cache placement, and offloading decisions are optimized for energy-efficient maximization. However, only one LEOSat is considered in this work. The authors in [17] have proposed a frequency-reuse-based bandwidth-sharing solution for the ISTNs to extend the coverage area. In this scheme, each satellite beam uses a specific frequency while the terrestrial cells in its coverage reuse the frequency bands from other beams, however, only power and bandwidth allocation are optimized. In [18], the authors considered an ISTN supporting IoT uplink transmission. The transmission process consists of two hops, e.g., IoT devices to the central earth stations (CETs) and from CETs to the LEOSat. This work aimed to optimize the RA to minimize the completion time of each hop separately. However, the work in [18] solely addressed the one-tier LEO-BS associations, yet it is essential to consider the end-to-end UE-BS-LEO performance comprehensively. In particular, the user data is transmitted through two hops, i.e., UE-BS-LEOSat, and the aggregated data throughputs at each BS and LEOSat are limited by the backhaul link capacity and bandwidth limitation. Therefore, one must optimize the RA for both UE-BS access and backhaul links and manage the two-tier UE-BS-LEO associations regarding the dynamics of satellite movements to balance the traffic at each BS and LEOSat and improve the end-to-end performance of an ISTN.

As a result, different two-tier association and RA solutions for the ISTNs have been studied in recent works [19], [20], [21], [22], [23], [24]. In [19], a novel joint offloading and user association solution was designed to maximize the total transmission rate for ISTNs supporting a disaster area that consists of a number of high-altitude-platforms (HAPs) and one LEOSat. In [20], a random access service for UEs in an ISTN is studied wherein every UE can choose either the BS or the LEOSat to associate with for data transmission. In this work, UE-BS association, bandwidth, and power allocation are optimized separately for maximizing the transmission rate of the UEs. Note that only one LEOSat is considered in the systems of [19] and [20]. Next, the ISTNs with multiple LEOSats were considered in [21] and [22]. Specifically, [21] aimed to maximize the sum rate and also the number of served UEs in an ISTN wherein the LEOSats provide the backhaul access service to TNs including a macro cell and several small cell BSs. To obtain the solution to this multiple-object optimization problem, two matching algorithms were proposed. In a different approaching way, the authors in [22] discussed how two network operators, i.e, satellite operator (SO) and terrestrial operator (TO), cooperate to provide the radio access services to a set of users effectively. To do so, a Stackelberg game was formulated based on which the user association, bandwidth allocation, and service price are optimized so that the revenue equilibrium can be achieved. However, it is worth noting that the transmit power has been kept unchanged and not optimized in both [21], [22]. Furthermore, all [19], [20], [21], [22] only focused on RA frameworks for the snapshot model at a specific time where the system dynamic has not been investigated. Particularly, the high mobility of the LEOSats leads to the dynamic of the system, especially the variance of backhaul link capacity between BSs and LEOSats. Therefore, the window-based model should be considered, where the system is considered within subsequent windows of time, capturing the dynamics of the systems.

Subsequently, the window-based model regarding LEOSat's movement within a number of time slots has been studied to develop dynamic RA mechanisms for the ISTNs in [23], [24], and [25]. The authors in [23] and [24] discussed how the LEOSats use Ka-band to provide the backhaul link to TNs proficiently. A three-dimensional LEO constellation optimization algorithm was proposed to minimize the number of satellites under the seamless coverage and backhaul capacity requirements over time windows. However, these works were analyzed without considering the RA at the UE-BS tier. Dai et al. [25] proposed two dynamic window-based greedy algorithms which handily address the user association and enlarge the coverage areas while maximizing the total network capacity. In this work, multiple frequency access and users' demand have been not considered. To the best of our knowledge, the joint design of two-tier UE-BS-LEO association, sub-channel assignment, bandwidth allocation, and power control for ISTNs over time regarding the user demand and limited-backhaul constraints have not been thoroughly studied in the literature. Specifically, different design aspects of the existing frameworks studying two-tier UE-BS-LEO are summarized in Table I. That motivates us to fill the gap in this paper.

TABLE I
SUMMARY OF WORKS

Works	Model	Sat. No.	Objective function	QoS	2T UA	SA	TN PC	NTN PC	BWA
Ref. [19]	Snapshot	1	Max sum-rate	Rate-threshold	✓	✗	✗	✗	✗
Ref. [20]	Snapshot	1	Max sum-rate	Rate-threshold	✓	✗	✓	✗	✓
Ref. [21]	Snapshot	Multiple	Max-rate & number of served UEs	None	✓	✓	✗	✓	✓
Ref. [22]	Snapshot	Multiple	Achieve the revenue equilibrium	None	✓	✗	✗	✗	✓
Ref. [24]	Snapshot	Multiple	Min number of used satellites	Global coverage	✓	✗	✗	✗	✗
Ref. [25]	Window-based	Multiple	Max sum-rate	None	✓	✗	✗	✓	✗
Our work	Window-based	Multiple	Min completion time	User demand	✓	✓	✓	✓	✓

SA: Sub-channel assignment TN PC: Power control in TNs 2T UA: Two-tier user association
NTN PC: Power control in NTNs BWA: Bandwidth allocation

B. Research Contributions

In this work, we study a time-window-based two-tier association and RA framework for the ISTNs. The data from UEs are forwarded to the LEO constellation systems through a two-hop transmission including terrestrial access links UE-BS and backhaul links BS-LEOSat. Regarding the quality of experience at UEs in terms of the data delivery time, this work aims to minimize the duration required to transfer all UEs' data to the LEO constellation. In this system, the technical issues encompassing UE-BS and BS-LEO associations, subchannel allocation, transmission power control, and bandwidth management are carefully addressed and designed to ensure optimal operation. The main contributions of this work can be summarized as follows:

- We study the window-based two-hop transmission model for LEO-based ISTNs under a practical system architecture, which features the dynamic topology and time-varying LEO-based backhaul link capacity. Regarding this, we develop a comprehensive problem optimizing the two-tier user association and RA jointly under the backhaul link capacity constraint. The objective is to offload all user data to the LEO constellation during the shortest duration. The optimization problem is formed as a challenging non-convex mixed-integer non-linear programming (MINLP) due to the combination of the discrete objective function, non-convex constraints, and coupling between binary and continuous variables.
- To deal with this difficult problem, we propose two efficient solutions by utilizing compressed-sensing and successive-convex-approximation methods, namely centralized and decentralized algorithms, which align two proposed network management approaches, respectively. In particular, for the performance purpose, we develop the centralized algorithm which can be executed at central network controller, however, it may pose critical issues of practical implementation.
- For the implementation purpose, we further develop the decentralized algorithm that enables resource management to be optimized distributedly at local controllers with limited signaling between them. Consequently, we discuss how the decentralized algorithm can be efficiently implemented in the practical systems.
- For comparison purposes, we introduce a greedy-based algorithm and adapt an existing framework to suit our design requirements. The numerical results with practical parameters show the superiority of the proposed algorithms compared to the two reference baselines. Furthermore, the small outcome gap between the centralized and decentralized solutions also confirms the effectiveness of distributed designs.

The preliminary result of this manuscript was presented in [1] where only the centralized approach and the simple simulation were discussed. The rest of this paper is organized as follows. Section II introduces the system model and problem formulation. In Section III, one proposes two centralized and decentralized solution approaches. Next, benchmark algorithms and complexity analysis are described in Section IV. Subsequently, the numerical results are presented in Section V which is followed by the conclusion given in Section VI.

II. System Model and Problem Formulation

This work aims to study RA designs for the uplink transmission of a two-tier ISTN, where satellites of an LEO constellation connect to some isolated terrestrial BSs to forward the data from ground UEs located in a specified geographical area to the core network. One assumes that the capacity of the feeder links between the gateways (GWs) and LEO is large enough, i.e., Q/V-band or optical [26], [27]; hence, this work only focuses on two-hop transmission from UEs to BSs, and from BSs to LEOSats. Let $\mathcal{N} \triangleq \{1, \ldots, N\}$ and $\mathcal{K} \triangleq \{1, \ldots, K\}$ be the sets of BSs and UEs, respectively. For convenient, we further denote $m-$th LEOSat, $n-$th BS and $k-$th UE as $\texttt{LEO}_m$, $\texttt{BS}_n$ and $\texttt{UE}_k$, respectively. A multiple-time-slot transmission model is considered, in which every UE, i.e., $\texttt{UE}_k$, intends to transmit a data amount of D_k bits to the core network through terrestrial access and LEO-provided backhaul links. Here, we also assume that the duration of one time-slot (TS) is T_S (s). Regarding the coverage pattern of the NTN, the beam coverage can be moving with the satellite or fixed on the earth [28]. To sake simplicity, the beam coverage is assumed to be moving with the LEOSat. Furthermore, to reduce the complexity, only the satellites in the constellation that can provide effective backhaul links to the BSs are considered. Herein, the backhaul link from an LEOSat to a BS is marked as effective if the BS's location is inside the 3-dB coverage of that satellite's beam pattern. In addition, one assumes that the beam pattern is fixed, i.e., without adaptive beamforming. Since LEOSats move, the set LEOSats having effective links to the BSs varies over time. Let $\mathcal{M}_t \triangleq \{1, \ldots, M_t\}$ be the set of such satellites in TS t. In this system, the connections between UEs to BSs are processed following the 5G-NR standard over the mid-bands, i.e., 1-6 GHz, while the BSs connect to LEOSats by using very-small-aperture-terminal (VSAT) antennas over the high-bands, e.g., Ka-band. In addition, the system is assumed to support delay-tolerant mechanisms. In particular, due to the dynamic of the system, especially the high mobility of LEO satellites [29], and the limitation of the system resource, link disruption can occur, i.e., temporary disconnection for certain UEs. Therefore, we assume that the system supports delay- and disruption-tolerant networking architecture, wherein each node can store the information and forward it later when the connectivity is restored [29], [30], [31]. On the other hand, the impact of link disruption and delay-requirement are discussed later in the numerical results.

A. Network Management Operation

A vision of ISTN architecture in this work is illustrated by Fig. 1. One assumes that the cellular BSs are deployed in clusters due to specific geographic conditions. In each cluster, a local controller (LC) is deployed which connects to all corresponding BSs through limited capacity links. Via these links, the control information can be exchanged based on which the transmission of BSs and UEs inside the cluster

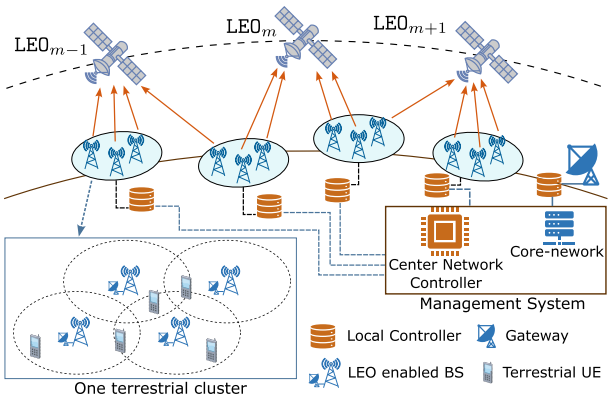

Fig. 1. System architecture of the ISTNs.

can be managed. On another side, the LEO constellation is operated by an NTN controller connecting to the GWs. In our vision, two network management structures can be considered for operating the cooperation between satellites and terrestrial networks, so-called centralized and decentralized.

- In the centralized structure, all LCs (including NTN one) are connected to a center network controller (CNC). This CNC can optimize all resource management functions, then, forward the controlling results to LCs for operation.
- In the decentralized structure, the distributed network operation can be processed by LCs with minimized information signaling among them via the central unit.

B. Channel Model

In this section, we discuss the channel models of the UE access links and the Ka-band backhaul links. The channel coefficient from $\mathtt{BS}_n$ to $\mathtt{LEO}_m$ is modeled as

$$\bar{g}_{m,n}[t] = \frac{\sqrt{G^{\mathtt{LEO}} G^{\mathtt{BS}} \psi(\theta_{m,n}) \mathrm{PL}^{\mathtt{NTN}}_{m,n}[t]}}{\varrho^{\mathsf{c}}_{m,n}[t] \varrho^{\mathsf{r}}_{m,n}[t]} e^{j2\pi(tT_S \nu^t_m - f_c d_{m,n}[t]/c)}, \quad (1)$$

where $\varrho^{\mathsf{c}}_{m,n}[t]$ and $\varrho^{\mathsf{r}}_{m,n}[t]$ stand for attenuation due to cloud and rain, $\mathrm{PL}^{\mathtt{NTN}}_{m,n}[t] = 1/(4\pi f_c d_{m,n}[t]/c)^2$ and $d_{m,n}[t]$ denote the free space path loss and the distance from $\mathtt{BS}_n$ to $\mathtt{LEO}_m$ at TS t; f_c and c are the operation frequency and light speed. $G^{\mathtt{LEO}}$ and $G^{\mathtt{BS}}$ are the antenna gains of the LEOSats and BSs. ν^t_m denotes the Doppler shift due to the mobility of $\mathtt{LEO}_m$ at TS t [32]. One assumes that the Doppler shift can be compensated at the LEOSat payload [30]. Moreover, $\psi(\theta)$ is the normalized beam pattern expressed in [28] as $\psi(\theta) = 1$ if $\theta = 0$, and $\psi(\theta) = 4\left|\frac{J_1(ba\sin\theta)}{ba\sin\theta}\right|$ if $\theta \neq 0$ where a is the antenna aperture, $J_1(\cdot)$ is the first-order Bessel function, $\theta_{m,n}$ is the boresight angle at the viewpoint of $\mathtt{LEO}_m$ to $\mathtt{BS}_n$, and $b = 2\pi f_c/c$. Besides, the channel coefficient of link $\mathtt{UE}_k - \mathtt{BS}_n$ over SC s at TS t is modeled as

$$\bar{h}_{n,k,s}[t] = \sqrt{\mathrm{PL}^{\mathtt{TN}}_{n,k}} \left(\sqrt{\frac{\kappa^{\mathtt{TN}}}{\kappa^{\mathtt{TN}}+1}} \bar{h}^{\mathtt{LOS}}_{n,k,s}[t] + \sqrt{\frac{1}{\kappa^{\mathtt{TN}}+1}} \bar{h}^{\mathtt{NLOS}}_{n,k,s}[t] \right), \quad (2)$$

where $\mathrm{PL}^{\mathtt{TN}}_{n,k}$ is the path-loss between $\mathtt{UE}_k$ and $\mathtt{BS}_n$, $\bar{h}^{\mathtt{LOS}}_{n,k,s}[t]$ and $\bar{h}^{\mathtt{NLOS}}_{n,k,s}[t]$ are the LOS and NLOS small scale falding of link $\mathtt{UE}_k - \mathtt{BS}_n$ over SC s at TS t, respectively. $\kappa^{\mathtt{TN}}$ is the Rician factor for the $\mathtt{UE} - \mathtt{BS}$ link. Additionally, the random-walk process is exploited to generate the *"time-correlation"* channels [33], [34], [35]. In particular, $\bar{h}^{\mathtt{NLOS}}_{n,k,s}[t]$ is generated as

$$\bar{h}^{\mathtt{NLOS}}_{n,k,s}[t] = (1-\rho)\bar{h}^{\mathtt{NLOS}}_{n,k,s}[t-1] + \rho\tilde{h}_{n,k,s}[t], \quad (3)$$

where $\bar{h}^{\mathtt{NLOS}}_{n,k,s}[0]$ and $\tilde{h}_{n,k,s}[t]$ are zero-mean unit-variance random variables, and ρ is the random-walk factor.

C. Transmission Over the Terrestrial UE-BS Access Links

Based on the 5G-NR standard, we assume that each UE can connect to at most one BS while each BS can serve multiple UEs at each TS. In addition, the transmission bandwidth (BW) for the terrestrial network is divided into S orthogonal sub-channels (SCs). Here, the BW of each SC is $W_{\mathtt{SC}} = 180 \times 2^{\mu}$ (kHz) where μ stands for the pre-selected numerology [36], [37]. The set of SCs is denoted by $\mathcal{S} \triangleq \{1, \ldots, S\}$. Regarding the UE-BS association and the SC allocation for UEs, we introduce a binary variable $\boldsymbol{\alpha}[t] \triangleq [\alpha_{n,k,s}[t]]_{\forall(n,k,s)}$ as

$$\alpha_{n,k,s}[t] = \begin{cases} 1, & \text{if } \mathtt{BS}_n \text{ serves } \mathtt{UE}_k \text{ over SC } s \text{ at TS } t, \\ 0, & \text{otherwise.} \end{cases} \quad (4)$$

In this scheme, an intra-cell orthogonal SC allocation strategy is assumed. It means that at every BS, each SC is assigned to at most one UE. This assumption is cast by the following,

$$(C1): \quad \sum_{\forall k \in \mathcal{K}} \alpha_{n,k,s}[t] \leq 1, \ \forall (n,s) \in (\mathcal{N} \times \mathcal{S}), \ \forall t. \quad (5)$$

Due to the limited computation resource, one assumes that $\mathtt{UE}_k$ can be assigned to at most $\bar{S}_k$ SCs at each TS, which yields

$$(C2): \quad \sum_{\forall s \in \mathcal{S}} \alpha_{n,k,s}[t] \leq \bar{S}_k, \ \forall (n,k) \in (\mathcal{N} \times \mathcal{K}), \ \forall t. \quad (6)$$

Moreover, the one-BS association constraint can be stated as

$$(C3): \sum_{\forall n \in \mathcal{N}} \Big\| \sum_{\forall s \in \mathcal{S}} \alpha_{n,k,s}[t] \Big\|_0 \leq 1, \ \forall k \in \mathcal{K}, \ \forall t. \quad (7)$$

Denote $p_{n,k,s}[t]$ as the transmit power from $\mathtt{UE}_k$ to $\mathtt{BS}_n$ over SC s, it can describe the received signal at $\mathtt{BS}_n$ over SC s as

$$y^{\mathtt{BS},t}_{n,s}(\mathbf{p}[t], \boldsymbol{\alpha}[t]) = \sum_{\forall (k,n')} \sqrt{\alpha_{n',k,s}[t] p_{n',k,s}[t]} \bar{h}_{n,k,s}[t] s_k + \eta_n, \quad (8)$$

where $\mathbf{p}[t] \triangleq [p_{n,k,s}[t]]_{\forall(n,k,s)}$, $s_k[t]$ is $\mathtt{UE}_k$'s data symbol, $\mathbb{E}\{|s_k[t]|^2\} = 1$, and $\eta_n \sim \mathcal{CN}(0, \sigma^2_n)$ is the additive Gaussian noise at $\mathtt{BS}_n$. Subsequently, the SINR of the $\mathtt{UE}_k$'s data received at $\mathtt{BS}_n$ over SC s and TS t can be expressed as

$$\gamma^{\mathtt{UE},t}_{n,k,s}(\mathbf{p}[t], \boldsymbol{\alpha}[t]) = \frac{\alpha_{n,k,s}[t] p_{n,k,s}[t] h_{n,k,s}[t]}{\sum_{\forall j \neq k} h_{n,j,s}[t] (\sum_{\forall i} \alpha_{i,j,s}[t] p_{i,j,s}[t]) + \sigma^2_n}, \quad (9)$$

where $h_{n,k,s}[t] = |\bar{h}_{n,k,s}[t]|^2$ is the corresponding channel gain. It is noting that, in (9), UEs that are not assigned SC s at $\mathtt{BS}_n$ do not cause the interference thanks to zero values of corresponding $\alpha_{n,k,s}[t]$. Let $W_{\mathtt{SC}}$ be the BW of one SC, we can describe $\mathtt{UE}_k$'s rate (nats/s) at $\mathtt{BS}_n$ over SC s as

$$R^{\mathtt{UE},t}_{n,k,s}(\mathbf{p}[t], \boldsymbol{\alpha}[t]) = W_{\mathtt{SC}} \ln(1 + \gamma^{\mathtt{UE},t}_{n,k,s}(\mathbf{p}[t], \boldsymbol{\alpha}[t])). \quad (10)$$

Then, the total achievable transmission data rate of $\mathtt{UE}_k$ in TS t can be written as

$$R^{\mathtt{UE},t}_{k}(\mathbf{p}[t], \boldsymbol{\alpha}[t]) = \sum_{\forall n \in \mathcal{N}} \sum_{\forall s \in \mathcal{S}} R^{\mathtt{UE},t}_{n,k,s}(\mathbf{p}[t], \boldsymbol{\alpha}[t]). \quad (11)$$

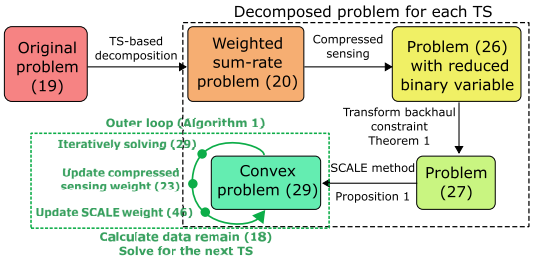

Fig. 2. Flowchart for the centralized solution.

D. Transmission Over the BS-LEOSat Backhaul Links

This subsection describes the transmission between the BS and the LEOSat. For convenience, the binary variables representing the BS-LEO association are introduced as

$$\mu_{m,n}[t] = \begin{cases} 1, & \texttt{BS}_n \text{ is served by } \texttt{LEO}_m \text{ at TS } t, \\ 0, & \text{otherwise.} \end{cases} \tag{12}$$

As described above, each BS can select at most one LEOSat at each TS to transmit the data, which yields

$$(C4): \quad \sum_{\forall m \in \mathcal{M}} \mu_{m,n}[t] \leq 1, \ \forall n \in \mathcal{N}. \tag{13}$$

Denote $W^{\texttt{BS}}_{m,n}[t]$ as a variable representing the BW allocation assigned to $\texttt{BS}_n$ for transferring data to $\texttt{LEO}_m$. Letting $\bar{W}^{\texttt{LEO}}_m[t]$ be the maximum BW at $\texttt{LEO}_m$ in TS t, we have

$$(C5): \sum_{\forall n \in \mathcal{N}} \mu_{m,n}[t] W^{\texttt{BS}}_{m,n}[t] \leq W^{\texttt{LEO}}_m[t], \ \forall (m,t). \tag{14}$$

Furthermore, high directivity VSAT antennas having a low side-lobe leakage are assumed at BSs based on which the inter-satellite interference can be ignored in this work [38]. Then, the achievable rate of $\texttt{BS}_n$ at $\texttt{LEO}_m$ in TS t is expressed as

$$R^{\texttt{BS},t}_{m,n}(\mathbf{P}[t],\mathbf{W}[t],\boldsymbol{\mu}[t]) = \mu_{m,n}[t] W^{\texttt{BS}}_{m,n}[t] \ln\left(1+\frac{P_n[t] g_{m,n}[t]}{W^{\texttt{BS}}_{m,n}[t]\delta_m}\right), \tag{15}$$

where $\mathbf{W}[t] \triangleq [W^{\texttt{BS}}_{m,n}[t]]_{\forall (m,n)}$, $\mathbf{P}[t] \triangleq [P_n[t]]_{\forall n}$, $P_n[t]$ denotes the transmit power of $\texttt{BS}_n$, $g_{m,n}[t] = |\bar{g}_{m,n}[t]|^2$ is the channel gain of link $\texttt{BS}_n - \texttt{LEO}_m$ in TS t, and δ_m is the noise power density at $\texttt{LEO}_m$. Therefore, the aggregated achievable rate of $\texttt{BS}_n$ at TS t is given as

$$R^{\texttt{BS},t}_{n}(\mathbf{P}[t],\mathbf{W}[t],\boldsymbol{\mu}[t]) = \sum_{\forall m \in \mathcal{M}} R^{\texttt{BS},t}_{m,n}(\mathbf{P}[t],\mathbf{W}[t],\boldsymbol{\mu}[t]). \tag{16}$$

Moreover, to ensure the successful forwarding at each BS, the total data rate of associated UEs needs to be less than the backhaul link capacity, which yields the following constraint

$$(C6): \sum_{\forall (k,s)} R^{\texttt{UE},t}_{n,k,s}(\mathbf{p}[t],\boldsymbol{\alpha}[t]) \leq R^{\texttt{BS},t}_{n}(\mathbf{P}[t],\mathbf{W}[t],\boldsymbol{\mu}[t]), \ \forall (n,t). \tag{17}$$

E. Problem Formulation

In this subsection, we formulate the optimization problem wherein the min-time objective is considered. It can be seen that, different from the terrestrial networks, the integrated LEOSat-terrestrial networks are highly dynamic due to the high movement of the LEOSats. The service time of BSs corresponding to one LEOSat is limited by its covering duration. As a result, the goal of this study is to develop a system that minimizes the time required to transfer the entire data of all UEs to the LEO constellation. To fulfill this technical objective, we first express the remaining data demand of $\texttt{UE}_k$ right after TS t as

$$d_k[t] = \max\left(0, D_k - \frac{T_S}{\ln 2} \sum_{u=1}^{t} R^{\texttt{UE},u}_k(\mathbf{p}[u],\boldsymbol{\alpha}[u])\right). \tag{18}$$

Thanks to (18), the joint two-tier association and RA design minimizing offloading duration for the ISTNs can be stated by the following optimization problem,

$$\begin{aligned} \min_{\mathbf{p},\mathbf{P},\mathbf{W},\boldsymbol{\alpha},\boldsymbol{\mu},v} \ & v \quad \text{s.t. constraints } (C1)-(C6), \\ & (C7): \sum_{\forall n \in \mathcal{N}} \sum_{\forall s \in \mathcal{S}} p_{n,k,s}[t] \leq p^{\max}_k, \ \forall k \in \mathcal{K}, \ \forall t \leq v, \\ & (C8): P_n[t] \leq P^{\max}_n, \ \forall n \in \mathcal{N}, \ \forall t \leq v, \\ & (C9): \alpha_{n,k,s}[t], \mu_{m,n}[t] \in \{0,1\}, \ \forall (m,n,k,s), \ \forall t \leq v, \\ & (C10): d_k[v] = 0, \ \forall k \in \mathcal{K}, \end{aligned} \tag{19}$$

where $\mathbf{p} \triangleq \{\mathbf{p}[t]\}_{\forall t}, \mathbf{P} \triangleq \{\mathbf{P}[t]\}_{\forall t}, \mathbf{W} \triangleq \{\mathbf{W}[t]\}_{\forall t}, \boldsymbol{\alpha} \triangleq \{\boldsymbol{\alpha}[t]\}_{\forall t}$ and $\boldsymbol{\mu} \triangleq \{\boldsymbol{\mu}[t]\}_{\forall t}$. Constraints $(C7)$ and $(C8)$ represent the corresponding limited transmission power of UEs and BSs, respectively. Variable v stands for the TS where all UE's data demands are completely transmitted as described by constraint $(C10)$. Regarding the goal of offloading duration minimization, v should be minimized.

In practical ISTNs, problem (19) aims to determine a resource management strategy to offload the entire UEs data to the core network through the satellite links during the shortest time. Particularly, the movement of LEOSats leads to the dynamic of the LEO-based backhaul link capacity and the network topology, which poses difficulties in resource management. The outcome by solving (19) can provide the solution of UE-BS and BS-LEOSat associations, SC assignment, BW allocation and power control at each TS to address these dynamic issues and minimize the transmission time. However, this problem consists of both continuous and binary variables, along with non-convex constraints associated with achievable rate formulas and limited link capacities, which forms it into a challenging MINLP problem. Hence, we propose the solutions to solve this problem in the next sections.

III. Proposed Solutions

Regarding two network management structures discussed in Section II-A, this section studies two frameworks to tackle the challenging problem (19) efficiently. The first solution operates solely at the CNC, whereas the latter is proposed to decompose the optimization process into sub-tasks that can be executed in parallel at the LCs. Both approaches utilize compressed sensing, relaxation, and approximation methods as follows.

A. Centralized Solution

The overall centralized solution approach is summarized in Fig. 2, in which the details will be given subsequently.

1) Time-Slot-Based Decomposition: It can be seen that the objective function brings the critical sparsity challenge to problem (19). Naturally, to upload all user demands in the shortest time, one should maximize the amount of transmitted data for each UE in every TS. Corresponding to the channel state in each TS, there is an achievable rate region for all UEs, i.e., $\mathcal{C}[t]$, which is the set of all possible rate vectors, $\left(R_1^{\mathtt{UE},t}(\mathbf{p}[t],\boldsymbol{\alpha}[t]),\ldots,R_K^{\mathtt{UE},t}(\mathbf{p}[t],\boldsymbol{\alpha}[t])\right)$. Regarding region $\mathcal{C}[t]$ and exploiting the approach presented in [39], [40], the window-based problem (19) can be transformed to a sequence of TS-based *"weighted sum-rate (SR) maximization"* problems each of which corresponds to a TS, e.g., TS t, as given follows,

$$\max_{\mathbf{p},\mathbf{P},\mathbf{W},\boldsymbol{\alpha},\boldsymbol{\mu}} \sum_{\forall(k,n,s)} \omega_k[t] R_{n,k,s}^{\mathtt{UE},t}(\mathbf{p}[t],\boldsymbol{\alpha}[t]) \text{ s.t. } (C1)\text{–}(C9). \tag{20}$$

Herein, $\omega_k[t]$ is a design weight corresponding to $\mathtt{UE}_k$'s remaining data in TS t.

Remark 1: To define the weight $\omega_k[t]$, one can consider the remaining data at every UE as a queuing model with no arrivals. Then, to upload all UE's data in the shortest time, the queue lengths of all UEs should reach zero at the same time after addressing the sequence of problems (20). Then, all queues need to be served in fairness, in other words, the queue length corresponding to all UEs, i.e., the data remaining of all UEs, needs to be kept equal over TSs. Based on ***Proposition 1*** *given in [39], one can achieve this goal by setting the weights to the queue lengths at each TS, i.e.,*

$$\omega_k[t] = d_k[t], \quad \forall(k,t). \tag{21}$$

Therefore, to tackle problem (19), one can sequentially solve problem (20) and update $\omega_k[t]$ after every TS until all UEs' data is uploaded to the LEO constellation successfully. Regarding TS t, it can be seen that problem (20) is still a non-convex MINLP owing to the coupling between binary and continuous variables, as well as the sparsity terms and the non-convex functions relating to SNR and SINR.

2) Compressed-Sensing-Based Relaxation: Regarding the relation between BS-UE association, SC assignment decision, and the continuous variables in TS t, one can see that:

- If $\mathtt{UE}_k$ is served by $\mathtt{BS}_n$ over SC s, the transmit power $p_{n,k,s}[t]$ is naturally positive, and vice versa, if $\mathtt{UE}_k$ is not served by $\mathtt{BS}_n$ over SC s, it should be $p_{n,k,s}[t]=0$.
- Similarly, for the LEO-BS association, if $\mathtt{BS}_n$ is served by $\mathtt{LEO}_m$, $W_{m,n}^{\mathtt{BS}}[t]$ is naturally positive, and vice versa, $W_{m,n}^{\mathtt{BS}}[t]=0$ if $\mathtt{BS}_n$ is not served by $\mathtt{LEO}_m$.

These observations yield the following results, $\alpha_{n,k,s}[t] = \left\|p_{n,k,s}[t]\right\|_0$, $\mu_{m,n}[t] = \left\|W_{m,n}^{\mathtt{BS}}[t]\right\|_0$, and

$$\left\|\sum_{\forall s}\alpha_{n,k,s}[t]\right\|_0 = \left\|\sum_{\forall s}p_{n,k,s}[t]\right\|_0 = \left\|p_{n,k}[t]\right\|_0, \tag{22}$$

for all (m,n,k,s,t), where $p_{n,k}[t]=\sum_{\forall s}p_{n,k,s}[t]$. Hence, $\boldsymbol{\alpha}$ and $\boldsymbol{\mu}$ can be represented by sparsity form of $\mathbf{p}$ and $\mathbf{W}$ efficiently. Subsequently, to address these sparsity terms, we tend to utilize an iterative compressed-sensing-based algorithm, so-called reweighted ℓ_1 minimization method [41], [42], which consists of the following process in each i^{th} iteration:

Algorithm 1 Proposed Centralized Algorithm

1: Set $t=1$.
2: **repeat**
3: **Initialization:** Set $i=0$, and generate an initial starting point $\left(\bar{\mathbf{p}}^{(0)}[t],(\mathbf{W}[t])^{(0)}\right)$.
4: **repeat**
5: Calculate SCALE weights $a_{n,k,s}^{(i)}, b_{n,k,s}^{(i)}$, compressed-sensing weights $\zeta_{n,k,s}^{(i)}, \xi_{n,k}^{(i)}, \chi_{m,n}^{(i)}$, and $\mathbf{p}^{(i)}[t] = \exp(\bar{\mathbf{p}}^{(i)}[t])$.
6: Solve (29) to obtain $\left(\bar{\mathbf{p}}^{\star}[t],\mathbf{P}^{\star}[t],\mathbf{W}^{\star}[t]\right)$.
7: Update $\left(\bar{\mathbf{p}}^{(i+1)[t]},\mathbf{W}^{(i+1)}[t]\right) := \left(\bar{\mathbf{p}}^{\star}[t],\mathbf{W}^{\star}[t]\right)$.
8: Set $i=i+1$.
9: **until** Convergence
10: Calculate $d_k[t],\forall k$ based on (18).
11: Set $t=t+1$.
12: **until** $d_k[t]=0,\forall k$.
13: Recovery association variables $\boldsymbol{\alpha}$ and $\boldsymbol{\mu}$ by (32).
14: **Output:** The solution $\left(\mathbf{p}^{\star},\mathbf{P}^{\star},\mathbf{W}^{\star},\boldsymbol{\alpha}^{\star},\boldsymbol{\mu}^{\star}\right)$.

(i) replacing the sparsity term $\|x\|_0$ by $1/\left(|x^{(i)}|^2+\epsilon\right)$ where ϵ is a small positive number; (ii) solving the approximate problem; (iii) updating the fixed point for the next iteration based on the recent achieved optimal solution. Employing this approach, ℓ_0-norm components in (22) can be approximated as

$$\begin{aligned}\left\|p_{n,k,s}[t]\right\|_0 &= \zeta_{n,k,s}^{(i)}[t]p_{n,k,s}[t], \left\|p_{n,k}[t]\right\|_0 \\ &= \xi_{n,k}^{(i)}[t]p_{n,k}[t], \\ \text{and } \left\|W_{m,n}^{\mathtt{BS}}[t]\right\|_0 &= \chi_{m,n}^{(i)}[t]W_{m,n}^{\mathtt{BS}}[t],\end{aligned} \tag{23}$$

for all (m,n,k,s,t), where $\zeta_{n,k,s}^{(i)}[t]$, $\xi_{n,k}^{(i)}[t]$ and $\chi_{m,n}^{(i)}[t]$ are the weights, which are updated based on the solution of $\mathbf{p}[t]$ and $\mathbf{W}[t]$ after the $(i-1)^{th}$ iteration, respectively as

$$\zeta_{n,k,s}^{(i)}[t]=\frac{1}{p_{n,k,s}^{(i-1)}[t]+\epsilon}, \xi_{n,k}^{(i)}[t]=\frac{1}{p_{n,k}^{(i-1)}[t]+\epsilon}, \chi_{m,n}^{(i)}[t]=\frac{1}{W_{m,n}^{\mathtt{BS},(i-1)}[t]+\epsilon}, \tag{24}$$

for all (m,n,k,s). Then, $(C1)-(C6)$ can be rewritten as

$$(\tilde{C}1): \sum_{\forall k\in\mathcal{K}} \zeta_{n,k,s}^{(i)}[t]p_{n,k,s}[t] \le 1, \ \forall(n,s), \tag{25a}$$

$$(\tilde{C}2): \sum_{\forall s\in\mathcal{S}} \zeta_{n,k,s}^{(i)}[t]p_{n,k,s}[t] \le \bar{S}_k, \ \forall(n,k), \tag{25b}$$

$$(\tilde{C}3): \sum_{\forall n\in\mathcal{N}} \xi_{n,k}^{(i)}[t] \sum_{\forall s\in\mathcal{S}} p_{n,k,s}[t] \le 1, \ \forall k, \tag{25c}$$

$$(\tilde{C}4): \sum_{\forall m\in\mathcal{M}_t} \chi_{m,n}^{(i)}[t]W_{m,n}^{\mathtt{BS}}[t] \le 1, \ \forall n, \tag{25d}$$

$$(\tilde{C}5): \sum_{\forall n\in\mathcal{N}} W_{m,n}^{\mathtt{BS}}[t] \le W_m^{\mathtt{LEO}}[t], \quad \forall m\in\mathcal{M}_t, \tag{25e}$$

$$(\tilde{C}6): \sum_{\forall(k,s)} R_{n,k,s}^{\mathtt{UE},t}(\mathbf{p}[t]) \le R_n^{\mathtt{BS},t}(\mathbf{P}[t],\mathbf{W}[t]), \ \forall n, \tag{25f}$$

where $\boldsymbol{\alpha}[t]$ and $\boldsymbol{\mu}[t]$ in $(C1)-(C6)$ are omitted.

Thanks to the compressed-sensing approach [41], problem (20) can be addressed by iteratively updating $\zeta_{n,k,s}^{(i)}[t]$ and $\chi_{m,n}^{(i)}[t]$, and solving the following problem

$$\max_{\mathbf{p},\mathbf{P},\mathbf{W}} \sum_{\forall(k,n,s)} \omega_k[t] R_{n,k,s}^{\mathtt{UE},t}(\mathbf{p}[t]) \text{ s.t.} (\tilde{C}1)-(\tilde{C}6),(C7),(C8). \tag{26}$$

Note that $R^{\mathrm{UE},t}_{n,k,s}(\mathbf{p}[t])$ and $R^{\mathrm{BS},t}_{n}(\mathbf{P}[t],\mathbf{W}[t])$ are the rate functions with omitting the arguments of $\boldsymbol{\alpha}[t]$ and $\boldsymbol{\mu}[t]$.

3) Convexifying Constraint ($\tilde{C}6$): It can be seen that problem (26) is still non-convex due to the non-convexity of $(\tilde{C}6)$. To address $(\tilde{C}6)$, we consider the following theorem.

Theorem 1: The solution for (26) can be obtained by solving the following problem,

$$\begin{aligned}\max_{\mathbf{p},\mathbf{P},\mathbf{W},\boldsymbol{\lambda}^{\mathrm{UE}},\boldsymbol{\lambda}^{\mathrm{BS}}}\ & \sum_{\forall k\in\mathcal{K}}\sum_{\forall n\in\mathcal{N}}\omega_k[t]\lambda^{\mathrm{UE}}_{n,k}[t] \qquad (27)\\ \text{s.t.}\ & \text{constraints } (\tilde{C}1)-(\tilde{C}5),(C7),(C8),\\ & (C11):\sum_{\forall k\in\mathcal{K}}\lambda^{\mathrm{UE}}_{n,k}[t]\le\lambda^{\mathrm{BS}}_{n}[t],\ \forall n,\\ & (C12):\lambda^{\mathrm{UE}}_{n,k}[t]\le\sum_{\forall s\in\mathcal{S}}R^{\mathrm{UE},t}_{n,k,s}(\mathbf{p}[t]),\ \forall(n,k),\\ & (C13):\lambda^{\mathrm{BS}}_{n}[t]\le\sum_{\forall m\in\mathcal{M}_t}R^{\mathrm{BS},t}_{m,n}(\mathbf{P}[t],\mathbf{W}[t]),\ \forall n,\end{aligned}$$

and calibrating $\mathbf{p}$ so that $(C12)$ holds with equality. Herein, $\boldsymbol{\lambda}^{\mathrm{UE}} \triangleq \{\lambda^{\mathrm{UE}}_{n,k}[t]\}$ and $\boldsymbol{\lambda}^{\mathrm{BS}} \triangleq \{\lambda^{\mathrm{BS}}_{n}[t]\}$ are new variables, which are introduced as a lower bound of the UE and BS transmission rate functions, respectively. Additionally, the $\mathbf{p}$-*calibrating process* can be done by solving the following problem,

$$\min_{\mathbf{p}}\ \sum_{\forall(n,k,s)}p_{n,k,s}[t]\ \text{s.t.}\ (\tilde{C}1)-(\tilde{C}3),(C7),(C12), \qquad (28)$$

which is well addressed in the literatures [43] and [44].

Proof: The proof is given briefly in Appenxdix A. ∎

Based on Theorem 1, we can tackle problem (26) by solving problem (27) and calibrating $\mathbf{p}$ by addressing (28) if $(C12)$ does not hold with equality. In the following, we will discuss how to deal with problem (27) efficiently.

4) Successive Convex Approximation for Low-complExity (SCALE) Method: It can be seen, (27) is non-convex due to constraint $(C12)$. To address this issue, one exploits the SCALE approach - a successive convex approximation method introduced in [43] and [45] - to transform the UE rate function into a concave form as follows.

Proposition 1: The equivalent problem of (27) at iteration $(i+1)$, TS t can be formulated as

$$\begin{aligned}\max_{\bar{\mathbf{p}},\mathbf{P},\mathbf{W},\boldsymbol{\lambda}^{\mathrm{UE}},\boldsymbol{\lambda}^{\mathrm{BS}}}\ & \sum_{\forall k\in\mathcal{K}}\sum_{\forall n\in\mathcal{N}}\omega_k[t]\lambda^{\mathrm{UE}}_{n,k}[t] \qquad (29)\\ \text{s.t.}\ & \text{constraints } (\tilde{C}4),(\tilde{C}5),(C8),(C11),(C13),\\ & (\bar{C}1):\sum_{\forall k\in\mathcal{K}}\zeta^{(i)}_{n,k,s}[t]\exp(\bar{p}_{n,k,s}[t])\le 1,\ \forall(n,s),\\ & (\bar{C}2):\sum_{\forall s\in\mathcal{S}}\zeta^{(i)}_{n,k,s}[t]\exp(\bar{p}_{n,k,s}[t])\le\bar{S}_k,\ \forall(n,k),\\ & (\bar{C}3):\sum_{\forall n}\xi^{(i)}_{n,k}[t]\sum_{\forall s}\exp(\bar{p}_{n,k,s}[t])\le 1,\ \forall k,\\ & (\bar{C}7):\sum_{\forall n\in\mathcal{N}}\sum_{\forall s\in\mathcal{S}}\exp(\bar{p}_{n,k,s}[t])\le p^{\max}_{k},\ \forall k,\\ & (\tilde{C}12):\lambda^{\mathrm{UE}}_{n,k}[t]\le\sum_{\forall s\in\mathcal{S}}\tilde{R}^{\mathrm{UE},t}_{n,k,s}(\bar{\mathbf{p}}[t]),\ \forall(n,k),\end{aligned}$$

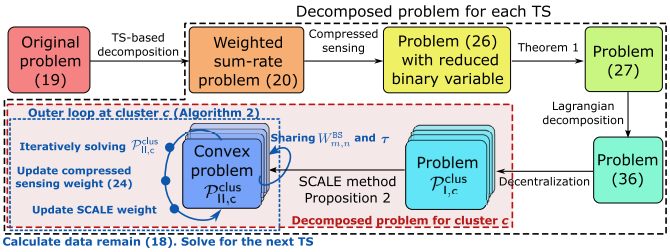

Fig. 3. Flowchart for the decentralized solution.

where $\bar{\mathbf{p}} \triangleq [\bar{\mathbf{p}}[t]]_{\forall t}$, $\bar{\mathbf{p}}[t] \triangleq [\bar{p}_{n,k,s}[t]]_{\forall(n,k,s)}$, $\bar{p}_{n,k,s}[t]$ is a new variable which is used instead of $p_{n,k,s}[t]$, and

$$\tilde{R}^{\mathrm{UE},t}_{n,k,s}(\bar{\mathbf{p}}[t]) = W_{\mathrm{SC}}\Big(a^{(i)}_{n,k,s}[t]\Psi^{t}_{n,k,s}(\bar{\mathbf{p}}[t]) + b^{(i)}_{n,k,s}[t]\Big), \qquad (30)$$

in which $a^{(i)}_{n,k,s}[t]$ and $b^{(i)}_{n,k,s}[t]$ are the updated coefficients at each iteration, and

$$\begin{aligned}\Psi^{t}_{n,k,s}(\bar{\mathbf{p}}[t]) = \ln(h_{n,k,s}[t]) + \bar{p}_{n,k,s}[t]\\ - \ln\Big(\sum_{\forall n'}\sum_{\forall k'\in\mathcal{K}\setminus k}h_{n,k',s}[t]e^{\bar{p}_{n',k',s}[t]}+\sigma^2_n\Big).\end{aligned} \qquad (31)$$

Proof: See Appendix B. ∎

Then, by exploiting the compressed-sensing and SCALE methods, as well as the valuable results addressed in the TS-based decomposition, Theorem 1, and Proposition 1, the solution for problem (19) can be obtained by iteratively solving problem (29) and updating the corresponding weights in every TS sequentially until all UEs' data have been delivered to LEO constellation. The proposed centralized algorithm is summarized in Algorithm 1. Regarding the compressed-sensing approach, the binary solution $\boldsymbol{\alpha}$ and $\boldsymbol{\mu}$ can be returned as

$$\begin{aligned}\alpha_{n,k,s}[t] &= \begin{cases}1, & \text{if } p_{n,k,s}[t]\ge\epsilon,\\ 0, & \text{otherwise,}\end{cases},\\ \mu_{m,n}[t] &= \begin{cases}1, & \text{if } W^{\mathrm{BS}}_{m,n}[t]\ge\epsilon,\\ 0, & \text{otherwise.}\end{cases}\end{aligned} \qquad (32)$$

B. Decentralized Solution

Implementing the centralized solution may pose a significant challenge, as it requires all network information to be available at the CNC. This requirement may lead to execution delays and an overload of controller links, arising from the aggregated traffic needed for exchanging network information. In addition, centralized execution also leads to computation overload and difficulties in scaling up the algorithm for large networks. Therefore, to address these issues - including overload at the central network controller, the large amount of exchanged network information, execution delays, and scalability concerns - a decentralized algorithm is proposed in this section. Subsequently, we decompose the centralized optimization process into sub-problems each of which can be solved separately at the corresponding LC. The overall decentralized solution approach is summarized in Fig. 3.

1) Lagrangian-Based Decomposition: Analyzing problem (27), one can see that the variable sets corresponding to clusters and NTN are coupled through constraint $(\tilde{C}5)$. To address this coupling, we propose to employ the Lagrangian relaxation method with the multiplexer $\boldsymbol{\tau} \triangleq [\tau_m[t]]_{\forall m,t>0}$ as follows. The Lagrangian function of (27) is given as

$$\begin{aligned} &L(\mathbf{p},\mathbf{P},\mathbf{W},\boldsymbol{\lambda}^{\mathtt{UE}},\boldsymbol{\lambda}^{\mathtt{BS}},\boldsymbol{\tau}) \\ &= \sum_{\forall(k,n)} \omega_k[t]\lambda^{\mathtt{UE}}_{n,k}[t] + \sum_{\forall m\in\mathcal{M}_t} \tau_m[t](\bar{W}^{\mathtt{LEO}}_m[t] - \sum_{\forall n\in\mathcal{N}} W^{\mathtt{BS}}_{m,n}[t]). \end{aligned} \tag{33}$$

Let Ω represent the tunnel of all variables, i.e., $\Omega \triangleq (\mathbf{p},\mathbf{P},\mathbf{W},\boldsymbol{\lambda}^{\mathtt{UE}},\boldsymbol{\lambda}^{\mathtt{BS}})$, $\mathcal{F}$ denote the feasible set of (27), i.e., $\mathcal{F} \triangleq \{\Omega | \Omega \text{ satisfies } (\tilde{C}1)-(\tilde{C}4),(C7),(C8),(C11)-(C13)\}$. The dual problem can be written as

$$\min_{\boldsymbol{\tau}} \; g_{\mathsf{Lag}}(\boldsymbol{\tau}) \text{ s. t. } \tau_m[t] \geq 0 \;\; \forall(m,t), \tag{34}$$

where $g_{\mathsf{Lag}}(\boldsymbol{\tau})$ is denoted as the dual function corresponding to (27) which is expressed as

$$\begin{aligned} &g_{\mathsf{Lag}}(\boldsymbol{\tau}) \\ &= \sup_{\Omega\in\mathcal{F}} L(\Omega,\boldsymbol{\tau}) \\ &= \sup_{\Omega\in\mathcal{F}} \Big(\sum_{\forall(k,n)} \omega_k[t]\lambda^{\mathtt{UE}}_{n,k}[t] + \sum_{\forall m\in\mathcal{M}_t} \tau_m[t](W^{\mathtt{LEO}}_m[t] - \sum_{\forall n\in\mathcal{N}} W^{\mathtt{BS}}_{m,n}[t]) \Big). \end{aligned} \tag{35}$$

For given $\boldsymbol{\tau}$ and $\{W^{\mathtt{LEO}}_m\}_{\forall m\in\mathcal{M}_t}$, the right-hand-side problem of (35) can be rewritten in a more trackable form as

$$\begin{aligned} \max_{\mathbf{p},\mathbf{P},\mathbf{W},\boldsymbol{\lambda}^{\mathtt{UE}},\boldsymbol{\lambda}^{\mathtt{BS}}} & \sum_{\forall(k,N)} \omega_k[t]\lambda^{\mathtt{UE}}_{n,k}[t] - \sum_{\forall m\in\mathcal{M}_t} \tau_m[t] \sum_{\forall n\in\mathcal{N}} W^{\mathtt{BS}}_{m,n}[t] \\ \text{s.t. } & (\tilde{C}1)-(\tilde{C}4),(C7),(C8),(C11)-(C13). \end{aligned} \tag{36}$$

Herein, for a decomposition purpose, we assume that the extra-cluster interference is negligible due to the sufficiently long distance between clusters. Based on this assumption, the optimization for the TN layer can be executed at each cluster. As a result, problem (36) can be further decomposed into sub-problems which are solved separately at the local control units corresponding to the clusters. In particular, the optimization sub-problem for cluster c is formulated as

$$\begin{aligned} &\big(\mathcal{P}^{\mathsf{clus}}_{\mathsf{l,c}}\big) \\ &\max_{\mathbf{p}_c,\mathbf{P}_c,\mathbf{W}_c,\boldsymbol{\lambda}^{\mathtt{UE}}_c,\boldsymbol{\lambda}^{\mathtt{BS}}_c} \sum_{\forall(k,n)} \omega_k[t]\lambda^{\mathtt{UE}}_{n,k}[t] - \sum_{\forall m\in\mathcal{M}_t} \tau_m[t] \sum_{\forall n\in\mathcal{N}_c} W^{\mathtt{BS}}_{m,n}[t] \\ &\quad \text{s.t. } (\tilde{C}1)_c-(\tilde{C}4)_c,(C7)_c,(C8)_c,(C11)_c,(C13)_c, \\ &\quad\quad (C14)_c: \lambda^{\mathtt{UE},c}_{n,k}[t] \leq \sum_{\forall s\in\mathcal{S}} R^{\mathtt{UE},c,t}_{n,k,s}(\mathbf{p}_c[t]), \;\; \forall(n,k), \end{aligned} \tag{37}$$

where the low suffix $(*)_c$ is added to notations (CX) and variables to indicate that constraint (CX) and corresponding variables are applied for cluster c. In constraint $(C14)_c$, $R^{\mathtt{UE},c,t}_{n,k,s}(\mathbf{p}_c[t]) = W_{\mathtt{SC}}\log_2(1+\gamma^{\mathtt{UE},c,t}_{n,k,s}(\mathbf{p}_c[t]))$, and

$$\gamma^{\mathtt{UE},c,t}_{n,k,s}(\mathbf{p}_c[t]) = \frac{p_{n,k,s}[t]h_{n,k,s}[t]}{\sum_{\forall n'}\sum_{\forall k'\in\mathcal{K}_c\setminus\{k\}} h_{n,k',s}[t]p_{n',k',s}[t] + I^{c,(i)}_{n,s} + \sigma^2_n}, \tag{38}$$

where $I^{c,(i)}_{n,s} = \sum_{\forall n'}\sum_{\forall j'\in\mathcal{K}\setminus\mathcal{K}_c} h_{n,j',s}[t]p^{(i)}_{n',j',s}[t]$ is the inter-cluster interference at BS n in cluster c over SC s.

2) Decentralized Algorithm: It can be seen that $(C14)_c$ is non-convex. The following proposition is to address this issue.

Proposition 2: Problem $\big(\mathcal{P}^{\mathsf{clus}}_{\mathsf{l,c}}\big)$ can be transformed into the following convex problem,

$$\begin{aligned} &\big(\mathcal{P}^{\mathsf{clus}}_{\mathsf{ll,c}}\big) \\ &\max_{\mathbf{p}_c,\mathbf{P}_c,\mathbf{W}_c,\boldsymbol{\lambda}^{\mathtt{UE}}_c,\boldsymbol{\lambda}^{\mathtt{BS}}_c} \sum_{\forall(k,n)} \omega_k[t]\lambda^{\mathtt{UE}}_{n,k}[t] - \sum_{\forall m\in\mathcal{M}_t} \tau_m[t] \sum_{\forall n\in\mathcal{N}_c} W^{\mathtt{BS}}_{m,n}[t] \\ &\quad \text{s.t. } (\bar{C}1)_c-(\bar{C}3)_c,(\tilde{C}4)_c,(\bar{C}7)_c,(C8)_c,(C11)_c,(C13)_c, \\ &\quad\quad (\bar{C}14)_c: \lambda^{\mathtt{UE}}_{n,k}[t] \leq W_{\mathtt{SC}} \sum_{\forall s\in\mathcal{S}} a^{(i)}_{n,k,s} \Psi^{c,t}_{n,k,s}(\bar{\mathbf{p}}_c[t]) + b^{(i)}_{n,k,s}, \end{aligned} \tag{39}$$

where $\Psi^{c,t}_{n,k,s}(\bar{\mathbf{p}}_c[t])$ is defined as

$$\begin{aligned} &\Psi^{c,t}_{n,k,s}(\bar{\mathbf{p}}_c[t]) \\ &\triangleq \ln(h_{n,k,s}[t]) + \bar{p}_{n,k,s}[t] \\ &\quad - \ln\Big(\sum_{\forall n'}\sum_{\forall k'\in\mathcal{K}_c\setminus k} h_{n,k',s}[t]\exp(\bar{p}_{n',k',s}[t]) + I^{c,(i)}_{n,s} + \sigma^2_n\Big). \end{aligned} \tag{40}$$

Proof: Using the similar approach described in Sub-Section III-A.3, $(C14)$ can be approximately convexified by utilizing function $a\ln(x)+b$. Then, $(C14)_c$ can be rewritten as $(\bar{C}14)_c$ with specific values of $a^{(i)}_{n,k,s}$, $\Psi^{c,t}_{n,k,s}(\bar{\mathbf{p}}_c[t])$, and $b^{(i)}_{n,k,s}$. Additionally, exploiting the same approach introducing the new variables $\bar{\mathbf{p}}_c[t] \triangleq [\bar{p}_{n,k,s}[t]]_{\forall(n,k,s)\in(\mathcal{N}_c\times\mathcal{K}_c\times\mathcal{S})}$, one can replace $(C1)_c-(C3)_c$ and $(C7)_c$ by $(\bar{C}1)_c-(\bar{C}3)_c$ and $(\bar{C}7)_c$, respectively. ∎

Remark 2: Due to the relatively long distance separating the clusters, the inter-cluster interference is assumed to be very minimal. Therefore, our decentralized design treats these inter-cluster interference components as fixed colored noise in each iteration. However, these terms are still re-estimated after each iteration to evaluate the SINR at the users precisely.

In sub-problem $\big(\mathcal{P}^{\mathsf{clus}}_{\mathsf{ll,c}}\big)$, the second term of the objective function, given in (39), can be considered as the balancing term corresponding to the LEO BW allocation. Herein, the parameter $\boldsymbol{\tau}$ needs to be adjusted to drive the solutions of all problems $\big(\mathcal{P}^{\mathsf{clus}}_{\mathsf{ll,c}}\big)$'s to meet constraint $(\tilde{C}5)$. One efficient conventional approach for this purpose is the use of the sub-gradient descent method [46]. In this method, the Lagrangian multiplier $\boldsymbol{\tau}$ can be updated as

$$\tau^{(\ell+1)}_m[t] = \tau^{(\ell)}_m[t] - \vartheta_\ell(W^{\mathtt{LEO}}_m - \sum_{\forall n\in\mathcal{N}} W^{\mathtt{BS}}_{m,n}), \tag{41}$$

where ϑ_ℓ is the step size. Moreover, this information will be disseminated to all LCs via a mechanism requiring limited signal transmission. The proposed decentralized algorithm is summarized in Algorithm 2. The convergence of this algorithm is discussed in the following.

Proposition 3: Regarding the dual problem, one have:

(i) The dual function g_{Lag} is a convex function.
(ii) Its sub-gradient at $\tau_m[t]$ is $W^{\mathtt{LEO}}_m - \sum_{\forall n\in\mathcal{N}} W^{\mathtt{BS}}_{m,n}$.
(iii) The sub-gradient updating method described in (41) is guaranteed to converge to the optimal solution of (34) if problem (36) is solved optimally and ϑ_ℓ's are set

Algorithm 2 Proposed Decentralized Algorithm

Set $t = 1$.
repeat
  Initialization: Set $\ell = 1$. Generate an initial Lagrangian multiplier $\boldsymbol{\tau}$.
  repeat
    for Each cluster c **do**
      Set $i = 0$ and select $\left(\bar{\mathbf{p}}_c^{(0)}[t], \mathbf{W}_c^{(0)}[t]\right)$.
      repeat
        Calculate weights $a_{n,k,s}^{(i)}, b_{n,k,s}^{(i)}, \zeta_{n,k,s}^{(i)}, \xi_{n,k}^{(i)}, \chi_{m,n}^{(i)}$ for cluster c and $\mathbf{p}_c^{(i)}[t] = \exp(\bar{\mathbf{p}}_c^{(i)}[t])$.
        Solve $\mathcal{P}_{\mathsf{II,c}}^{\mathsf{clus}}$ to obtain $\left(\bar{\mathbf{p}}_c^{\star}[t], \mathbf{P}_c^{\star}[t], \mathbf{W}_c^{\star}[t]\right)$.
        Update $\left(\bar{\mathbf{p}}_c^{(i+1)}[t], \mathbf{W}_c^{(i+1)}[t]\right) := \left(\bar{\mathbf{p}}_c^{\star}[t], \mathbf{W}_c^{\star}[t]\right)$.
        Set $i = i + 1$.
      until Convergence
    end for
    Update $\boldsymbol{\tau}$ by (41).
    Set $\ell = \ell + 1$.
  until Convergence
  Calculate $d_k[t], \forall k$ based on (18).
  Set $t = t + 1$.
until $d_k[t] = 0, \forall k$.
Recovery association variables $\boldsymbol{\alpha}$ and $\boldsymbol{\mu}$ by (32).
Output: The solution $\left(\mathbf{p}^{\star}, \mathbf{P}^{\star}, \mathbf{W}^{\star}, \boldsymbol{\alpha}^{\star}, \boldsymbol{\mu}^{\star}\right)$.

according to *"the square summable but not summable step size rule"* [46].

(iv) Once, the conditions given in (iii) are satisfied, the convergence rate of the sub-gradient method is $\mathcal{O}(1/\sqrt{\ell})$.

Proof: The proposition can be proved briefly based on the results described in [46] and [47] as follows:

(i) It can be seen that $g_{\mathsf{Lag}}(\boldsymbol{\tau})$ is the pointwise supremum of a family of affine functions, $g_{\mathsf{Lag}}(\boldsymbol{\tau})$ is convex [47].

(ii) The choice of $W_m^{\mathsf{LEO}} - \sum_{\forall n \in \mathcal{N}} W_{m,n}^{\mathsf{BS}}$ as the sub-gradient for $\tau_m[t]$ is justified by the fact that $\tau_m[t]$ is the Lagrangian multiplier associated with the constraint $(\tilde{C}5)$.

(iii) Due to the results given in Section 2 of [46], the above sub-gradient method is guaranteed the convergence if the step sizes are set according to *"the square summable but not summable step size rule"* such as $\vartheta_\ell = 1/\ell$.

(iv) Using the sub-gradient descent method to solve the dual problem; hence, its convergence rate is $\mathcal{O}(1/\sqrt{\ell})$ [46]. ■

Moreover, the duality gap is discussed in the following remark and proposition.

Remark 3: The strong duality does not hold for the dual problem (34) and the corresponding primal problem (27) since (27) is non-convex. It is important to highlight that the use of Lagrangian decomposition enables the parallel optimization execution across local clusters, helping to overcome the challenges in the centralized solution implementation related to the overload of controller links, execution delays, and scalability.

Proposition 4: Let $(\mathcal{P}_{\mathsf{II}})$ and $(\mathcal{D}_{\mathsf{II}})$ be the aggregation of all $(\mathcal{P}_{\mathsf{II,c}}^{\mathsf{clus}})$'s and its dual problem, respectively. If the inter-cluster interference is neglectable, i.e., $I_{n,s}^c \approx 0$, the strong duality holds for $(\mathcal{P}_{\mathsf{II}})$ and problem (29) in the centralized algorithm.

Proof: See Appendix C. ■

Remark 4: Thanks to Proposition 3, if the problems $\left(\mathcal{P}_{\mathsf{I,c}}^{\mathsf{clus}}\right)$ *are solved optimally and the Lagrangian variables* $\boldsymbol{\tau}$ *are updated as in (41) based on the bandwidth allocation solution* $\mathbf{W}$*, the convergence of the decentralized algorithm can be guaranteed. The strategy for exchanging and updating the Lagrangian variables* $\boldsymbol{\tau}$ *will be discussed in the subsequent section. Although Algorithm 2 may not obtain the optimal solution of* $\mathbf{W}$ *in each iteration due to the approximation attempt, the implementation of compressed sensing and SCALE methods in this algorithm–well-known as highly effective tools for dealing with sparsity and non-convex sum logarithm-rate maximization problems–can facilitate an efficient solution. Consequently, the convergence of Algorithm 2 is feasible, as demonstrated in Section V. Furthermore, the distributed algorithm can be also set to stop after a certain number of iterations in a practical implementation.*

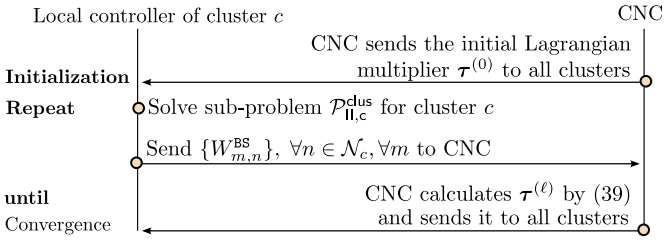

Fig. 4. Exchange data between local cluster controllers and CNC.

3) Decentralized Algorithm Implementation With Limited Signaling: To provide clarity on the practical implementation, Fig. 4 is presented to outline the execution steps and data exchange between the cluster LCs and CNC. Specifically, the process can be summarized as follows:

(a) After obtaining the initial Lagrangian multiplier $\boldsymbol{\tau}^{(0)}$ each cluster LC solves its corresponding sub-problem as described in Algorithm 2.
(b) Subsequently, the cluster LCs and the central control unit exchange the data of BW allocation that is used for Lagrangian multiplier calculation.
(c) The CNC calculates and broadcasts the new $\boldsymbol{\tau}$ to all LCs.

This process is reiterated until the convergence of the solution is attained. Moreover, as depicted in Fig. 1, one assumes the existence of a limited-capacity link between every LC and the CNC. Given the low-bit exchanging data ($W_{m,n}^{\mathsf{BS}}$ and $\tau^{(\ell)}$), the signaling process can be carried out with low latency.

Remark 5: Two proposed algorithms are designed based on the min-time optimization problem (19), however, they can easily adapt to the max-sum-rate objective with a simple modification. Indeed, by removing the weights ω_k *at the objective functions of (29) and sub-problems* $\mathcal{P}_{\mathsf{II,c}}^{\mathsf{clus}}$*, the proposed centralized algorithm and decentralized algorithm can directly apply to solve the max-sum-rate optimization problem.*

IV. Other Solutions and Complexity Analysis

A. Greedy Algorithm

Regarding BS-LEO links in each TS, each BS selects an LEOSat having the strongest channel gain for communication. Consequently, every LEOSat assigns equal BW to its associated BSs. Every BS spends all its power budget to forward UEs data, based on which the backhaul capacity R_n^{BS} of the BSs is defined. Then, in every TS, one updates the set of

Algorithm 3 Greedy-Based Algorithm to Solve (19)

Set $t = 1$ and $\mathcal{K}_{\mathtt{D}} = \mathcal{K}$.
repeat
  for $n = 1 \rightarrow N$ **do**
    $\mathtt{BS}_n$ associates with $\mathtt{LEO}_m$ with the best channel gain. Set $\mu_{m,n} = 1$ and $P_n[t] := P_n^{\max}$.
  end for
  Each LEOSat uniformly allocates BW to linked BSs.
  Each $\mathtt{UE}_k \in \mathcal{K}_{\mathtt{D}}$ selects $\mathtt{BS}_n$ with the best channel gain.
  Each BS assigns SCs to UEs in descending order of channel gain.
  Build matrix $\boldsymbol{\alpha}$. Set $\bar{p}_{\mathtt{UE}}^{\max} = p_{\mathtt{UE}}^{\max}$.
  for $n = 1 \rightarrow N$ **do**
    while $R_n^{\mathtt{BS}} < R_n^{\mathtt{total}}$ or $|R_n^{\mathtt{BS}} - R_n^{\mathtt{total}}| > \epsilon_{\mathsf{rate}}$. **do**
      Utilize water-filling algorithm for each UE linked with $\mathtt{BS}_n$ to find power allocation using $\bar{p}_{\mathtt{UE}}^{\max}$ as the maximum power.
      Adjust $\bar{p}_{\mathtt{UE}}^{\max}$ by bisection search method based on $R_n^{\mathtt{total}}$.
    end while
  end for
  Calculate $d_k[t], \forall k$ based on (18).
  $\forall k \in \mathcal{K}_{\mathtt{D}}$, remove $\mathtt{UE}_k$ with $d_l[t] = 0$: $\mathcal{K}_{\mathtt{D}} = \mathcal{K}_{\mathtt{D}} - \{k\}$.
  Set $t = t + 1$.
until $\mathcal{K}_{\mathtt{D}} = \emptyset$.
Output: The solution $(\mathbf{p}, \mathbf{P}, \mathbf{W}, \boldsymbol{\alpha}, \boldsymbol{\mu})$.

UEs asking for data transmission, i.e., $\mathcal{K}_{\mathtt{D}}$. Then, each UE in $\mathcal{K}_{\mathtt{D}}$ selects the BS offering the best average channel gain to associate with. At the BSs, SCs are assigned to the UEs in descending order of channel gain. Afterward, the water-filling algorithm is employed to optimize the transmission power at UEs without considering extra-cell interference. Herein, the maximum auxiliary power level at UEs needs to be calibrated if the capacity constraints of the BS-LEOSat backhaul link is violated. The Greedy Algorithm is detailed in Algorithm 3, wherein $R_n^{\mathtt{total}}$ is the total UE rate at $\mathtt{BS}_n$.

B. Other Benchmark Solution

As shown in Table I, Di et al. [21] studied some technical aspects similar to our work without optimizing the transmission power at UEs. However, [21] allocates only one sub-channel to each UE, letting each BS connect to multiple LEOSats at the same time, and accounting for inter-satellite interference which may be impractical in VSAT systems. Then, we aim to modify the algorithm proposed in [21], namely Di Algorithm, for a fair evaluation. The main modifications are: (i) allowing UEs to be assigned $\bar{S}$ SCs; (ii) equally allocating the transmission power at each UE over its assigned SCs; (iii) pushing each BS to connect to only one LEOSat; (iv) ignoring the inter-satellite interference, then utilizing the water-filling method to allocate power transmission for BSs.

C. Complexity Analysis

1) Greedy Algorithm: Regarding Algorithm 3, the FOR loop given in **Steps 3-5**, the BW allocation procedure in **Step 6**, and BS-UE association operation in **Step 7** demand a complexity of $\mathcal{O}(2N+K)$. Then, the complexity of SC assignment process in **Step 8** is $\mathcal{O}(NS)$. For the power allocation work given in **Steps 10-15**, one requires $-\log_2(\epsilon_{\mathsf{pow}})$ and $-\log_2(\epsilon_{\mathsf{rate}})$ iterations to find $\bar{p}_{\mathtt{UE}}^{\max}$ level and water level by bisection search method, respectively. Additionally, the complexities of obtaining UE power control and calculating the data remaining are $\mathcal{O}(NK\bar{S})$ and $\mathcal{O}(K)$ computations, respectively. In summary, the complexity of the greedy algorithm can be expressed as

$$X_{\mathsf{Gre.Alg.}} = \mathcal{O}\Big(T^{\mathsf{Gre}} NK\bar{S} \log_2(\epsilon_{\mathsf{rate}}) \log_2(\epsilon_{\mathsf{pow}})\Big), \quad (42)$$

where T^{Gre} is the number of TS required for uploading all UE data of the greedy algorithm.

2) Di Algorithm: In Di Algorithm, the most computation complexity is due to the three-dimension matching process. In particular, a three-dimension matching approach is utilized for the BS-UE-SC association repeatedly to let each UE can access multiple SCs from one BS, this process demands a complexity of $\mathcal{O}(NK^2S^2\bar{S})$. For the BS-LEOSat transmission, the three-dimension matching approach is applied again for the LEOSat-BS-SC association to let each BS can connect to one LEOSat over at most $\bar{S}_{\mathtt{BS}}$ SCs. The complexity of this process can be expressed as $\mathcal{O}(MN^2S_{\mathtt{LEO}}^2\bar{S}_{\mathtt{BS}})$, where $S_{\mathtt{LEO}}$ is the number SCs in the LEOSat-BS transmission. In summary, the complexity in terms of big-O of Di Algorithm can be expressed as

$$X_{\mathsf{Di.Alg.}} = \mathcal{O}\Big(N_{\mathsf{out}}(NK^2S^2\bar{S} + MN^2S_{\mathtt{LEO}}^2\bar{S}_{\mathtt{BS}})\Big), \quad (43)$$

where N_{out} is the number of outer iterations for convergence.

3) Proposed Algorithms: Each proposed algorithm consists of two loops: the outer loop corresponds to the number of TSs of transmission required for completing the upload of all UEs data while the inner loop iteratively solves the optimization problems until the solution for each TS is obtained. To implement each algorithm, the successive convex problems (29) and (39) should be transformed into the conic form which is accepted by the convex solvers, e.g., MOSEK [48], [49], resulting in requires extra constraints and auxiliary variables. Regarding the centralized algorithm, one needs to deal with problem (29) several times. According to [49], this problem can be transformed into a conic problem which consists of $x_1 = NKS + NS + NK + 4N + 2K + M_t$ linear constraints, $y_1 = N^2K^2S + 2NKS + M_tN$ exponential cone constraints, and $z_1 = N^2K^2S + 4NKS + NK + 3M_tN + N$ variables. Based on [49] and [50], to obtain ϵ-accuracy solution for problem (29), the connect-based solving procedure requires a number of $\mathcal{O}\Big(3\log(1/\epsilon)\Big)$ sub-steps. Therefore, the complexity of the centralized algorithm can be expressed as

$$X_{\mathsf{Cen}} = \mathcal{O}\Big(9T^{\mathsf{Cen}}N_{\mathsf{iter}}\log(1/\epsilon)\Big((2(z_1+1)+x_1)^3+y_1\Big)\Big), \quad (44)$$

where N_{iter} is the number of inner-loop iterations, T^{Cen} is the required number of TSs due to the centralized algorithm.

For the decentralized algorithm, it is equivalent to a conic problem with $x_2 = N_cK_cS + N_cS + N_cK_c + 4N_c + 2K_c + M_t$ linear constraints, $y_2 = N_c^2K_c^2S + 2N_cK_cS + M_tN_c$ conic constraints, and $z_2 = N_c^2K_c^2S + 4N_cK_cS + N_cK_c + 3M_tN_c + N_c$ variables. Therefore, its complexity can be written as

$$X_{\mathsf{Dec}} = \mathcal{O}\Big(9T^{\mathsf{Dec}}N_{\mathsf{iter}}N_{\mathsf{Lag}}\log(1/\epsilon)\Big((2(z_2+1)+x_2)^3+y_2\Big)\Big), \quad (45)$$

TABLE II
SIMULATION PARAMETERS

Parameter	Value	Parameter	Value
Number of BS clusters	6	LEOSat BW, W^{LEO}	20 MHz
Number of UEs, K	60	Orbit type	Walker-star
Number of BSs, N	18	Number of BSs per cluster	3
LEOSat altitude	600 km	LEOSat velocity	7.57 km/s
Number of satellite orbits	2	LEOSat antenna gain, G^{LEO}	37.1 dBi
UE data demand, $\bar{D}$	5 Mbits	SC BW, W_{SC}	720 kHz ($\mu = 2$)
BS antenna gain, G^{BS}	32.8 dBi	BS-LEO operation frequency, f_c	30 GHz
Number of SCs, S	8	Max. number of SCs at UE, $\bar{S}$	4
TS duration, T_S	30 ms	Max. UE transmit power, $p_{\text{UE}}^{\max}$	26 dBm
Rician κ factor, κ^{TN}	5 dB	Max. BS transmit power, $P_{\text{BS}}^{\max}$	14 dBW
Radius of TN cell	200 m	Considered area	(7km × 5km)
Satellite 3dB beam diameter	12.35 km	Noise power density	-174 dBm/Hz

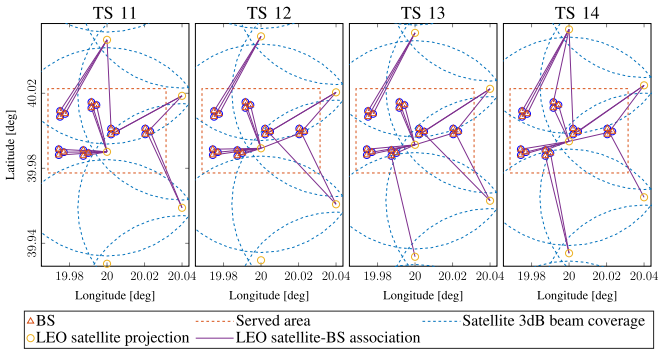

Fig. 5. The LEOSat-BS association result over TSs.

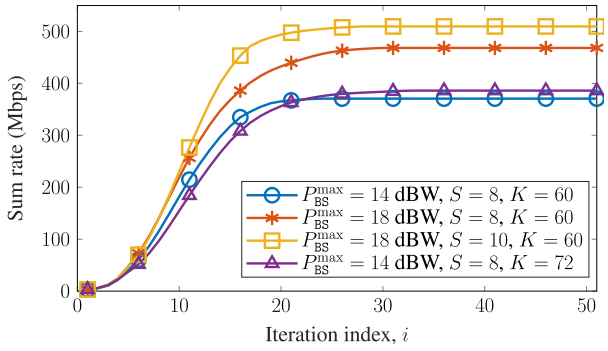

Fig. 6. Sum-rate of the centralized algorithm in TS 1 over iterations.

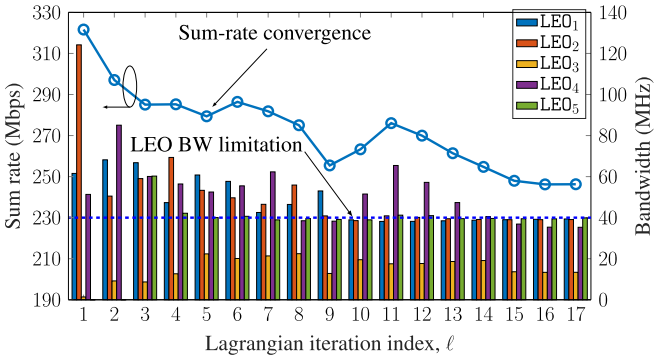

Fig. 7. Sum-rate and BW of proposed *Dec-Alg* in TS 1 over iterations.

where N_{Lag} is the number of Lagrangian iterations, T^{Dec} is the required number of TSs due to the decentralized algorithm. Here, both algorithms have polynomial time complexities while the decentralized approach has a lower complexity.

V. NUMERICAL RESULTS

A. Setting Parameters

This section presents the simulation results to evaluate the performance of the proposed solutions and compare them with reference algorithms. The simulations were performed over an area of 7×5 km^2, with the center geographical coordinate set at $(\varphi_0, \theta_0) = (40°\text{N}, 20°\text{E})$. Within this area, terrestrial clusters were uniformly deployed and CNC is assumed to be located at the center of the area. The rain attenuation $\varrho_{m,n}^{\text{c}}[t]$ is assumed to follow "log-normal distribution" with a mean of 2.6 dB and a variance of 1.63 dB [51], while the cloud attenuation $\varrho_{m,n}^{\text{r}}[t]$ is set as detailed in [52]. The Doppler shift, ν_m^t, is calculated based on LEOSat velocity and position as described in [53]. Other key parameters are listed in Table II. To ease the readability, two proposed algorithms, i.e., Algorithm 1 and Algorithm 2 are referred to as *"Cen-Alg"* and *"Dec-Alg"*, respectively. The Greedy Algorithm and Di Algorithm are also implemented for comparison purposes.

B. Numerical Results

Fig. 5 displays a simulated topology along with the LEOSat-BS association results, as obtained from the proposed *Cen-Alg* during the duration from TS 11 to TS 14, wherein the satellite 3dB beam coverage is calculated based on beam pattern formulation given in Section II-B and parameters in Table II. It can be observed that BSs in the service area tend to prioritize connection with the nearest LEOSat due to the strong channel gain (the middle LEOSat in Fig. 5). However, due to limited backhaul capacity, several BSs connect to distant LEOSats. Moreover, it can be seen that LEO switching does not occur too frequently. Specifically, in this duration, there are a few BSs that need to switch their LEO association.

Fig. 6 illustrates the SR achieved by the proposed *Cen-Alg* over iterations in TS 1 for different settings. As can be observed, in all settings, the achieved SR increases and saturates after just a few tens of iterations, that has confirmed the convergence of our proposed *Cen-Alg*. For instance, with the settings of $(P_{\text{BS}}^{\max}, S, K) = (14, 8, 60)$ and $(P_{\text{BS}}^{\max}, S, K) = (18, 8, 60)$, our proposed *Cen-Alg* requires approximately 23 and 26 iterations for convergence, respectively. Even with a larger setting, $(P_{\text{BS}}^{\max}, S, K) = (18, 8, 60)$ and $(P_{\text{BS}}^{\max}, S, K) = (14, 8, 72)$, a similar number of iterations for convergence is required, i.e., about 28 and 27 iterations, respectively.

Fig. 7 depicts the SR convergence and the allocated BW of each LEOSat over Lagrangian iterations. In this approach, at each Lagrangian iteration, each cluster solves a sub-problem similar to the problem addressed in the centralized approach, but on a smaller scale. Therefore, the SR convergence of the *Dec-Alg* at each cluster can be achieved with a lower number of iterations in comparison to that of the proposed *Cen-Alg*. In this instance, the proposed *Dec-Alg* requires approximately 15 Lagrangian iterations for convergence. Intriguingly, during the initial iterations, the algorithm delivers superior SR performance, but there are some LEOSats where the total allocated BW exceeds the maximum BW at the LEOSat (indicated by the threshold dashed line). This phenomenon occurs due to the relaxation of the BW constraint at each LEOSat. However, thanks to the adjustment of the Lagrangian multiplier $\boldsymbol{\tau}$ based on (41), the BW violation decreases in

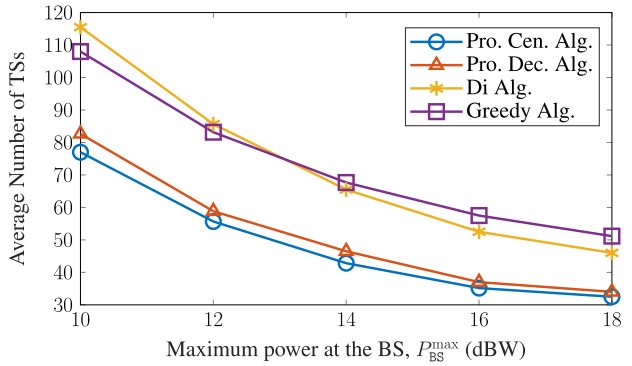

Fig. 8. Average TS number vs. BS max power.

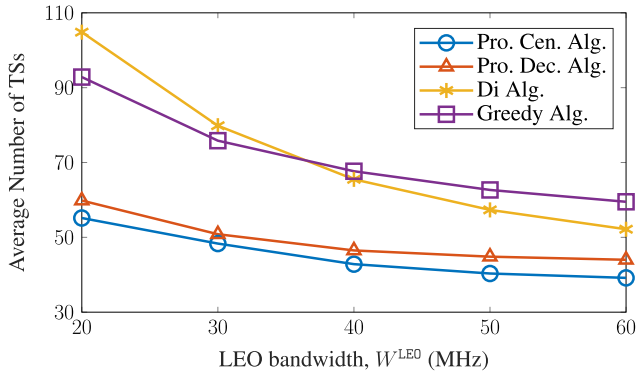

Fig. 9. Average TS number vs. LEO BW.

later Lagrangian iterations, and the BW allocation constraint is fulfilled upon achieving convergence.

To assess the effect of backhaul link capacity, Fig. 8 depicts the average numbers of TSs required to meet UE demand according to the four algorithms versus different maximum BS power levels. Overall, the results of all algorithms share the same trend that the average TS number decreases as the maximum BS transmission power increases. As anticipated, both proposed algorithms outperform the benchmarks with considerable performance gaps. For instance, at $P_{\text{BS}}^{\max} = 12$ dBW, the average numbers of TSs required to meet UE demand for the two proposed algorithms are approximately 55.7 and 58.8 TSs. In contrast, the Di Algorithm and the Greedy Algorithm require substantially more TSs, specifically around 85.6 and 83.2 TSs, respectively. Across all settings of $P_{\text{BS}}^{\max}$, the gap between the proposed algorithm and the benchmark lines seems to be unchanged, i.e., approximately 30 TSs. Particularly noteworthy is the minor performance gap between the *Cen-Alg* and *Dec-Alg*, roundly about 3 TSs, even though the latter algorithm is executed separately at the LCs.

To further evaluate the influence of the backhaul link capacity, Fig. 9 illustrates the performance of the four algorithms in terms of the average number of TSs versus the maximum backhaul BW which can be provided by the LEOSats. The trend of the results in this figure is similar to that shown in Fig. 8, where the average number of TSs decreases as the backhaul capacity budget increases. As can be seen, the two proposed algorithms deliver superior performance in terms of transmission time compared to the Di Algorithm and the Greedy Algorithm. For instance, at $W^{\text{LEO}} = 40$ MHz,

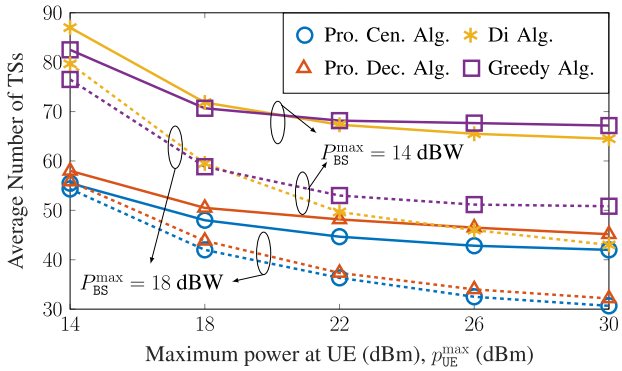

Fig. 10. The number of required TSs vs. the maximum power at UE.

the proposed *Cen-Alg* and *Dec-Alg* require approximately 42.8 and 46.5 TSs to fulfill UE demand, while the benchmark algorithms require about 65.5 and 67.6 TSs, respectively. Contrary to the results in Fig. 8, the performance gap between the proposed algorithms and the two benchmark algorithms is larger with a smaller W^{LEO}. This phenomenon demonstrates the efficiency and capability of the two proposed algorithms to exploit LEOSat BW compared to the benchmarks.

Subsequently, Fig. 10 illustrates the average number of TSs as a function of the UE transmission power budget. Again, the two proposed algorithms consistently provide superior solutions with a significant performance gap compared to the benchmarks. With $P_{\text{BS}}^{\max} = 14$ dBW, the Di Algorithm and the Greedy Algorithm require about 71.5 and 70.6 TSs, respectively, while the proposed algorithms require only approximately 48 and 50.5 TSs at $p_{\text{UE}}^{\max} = 18$ dBm. These numbers of TSs are reduced to about $64.5, 67.2, 42$ and 45.2 TSs at $p_{\text{UE}}^{\max} = 30$ dBm, respectively. Interestingly, the numbers of TSs corresponding to the four schemes decrease quickly when $p_{\text{UE}}^{\max}$ varies from 14 dBm to 18 dBm, but saturate when $p_{\text{UE}}^{\max}$ is set to a higher value. This indicates that the performance seems to be bottlenecked by the backhaul link capacity. For a clearer assessment, we examine the setting with $P_{\text{BS}}^{\max} = 18$ dBW. As expected, the number of TSs for the four algorithms decreases significantly as $p_{\text{UE}}^{\max}$ increases. When $p_{\text{UE}}^{\max}$ is set in the range from 22 dBm to 30 dBm, the performance of the Di Algorithm improves rapidly compared to that of the Greedy Algorithm. However, the performance gap remains substantial compared to the two proposed algorithms. In particular, the average numbers of TSs for the benchmarks are about 43 and 50.8 TSs, respectively, whereas those for the proposed algorithms are only 30.6 and 32.1 TSs at $p_{\text{UE}}^{\max} = 30$ dBm.

Next, Fig. 11 illustrates the impact of the number of SCs on the system performance in terms of the complete time of UE data upload. With $P_{\text{BS}}^{\max} = 14$ dBW, the benchmark algorithms require a similar number of TSs across all different settings of S, and this transmission time is much larger than those of the two proposed algorithms. Specifically, the proposed algorithms can reduce the requirement by approximately 23 and 21.5 TSs for all values of S in this simulation. Conversely, it can be seen that the average number of TSs achieved by all four schemes decreases slowly as the number of SCs increases.

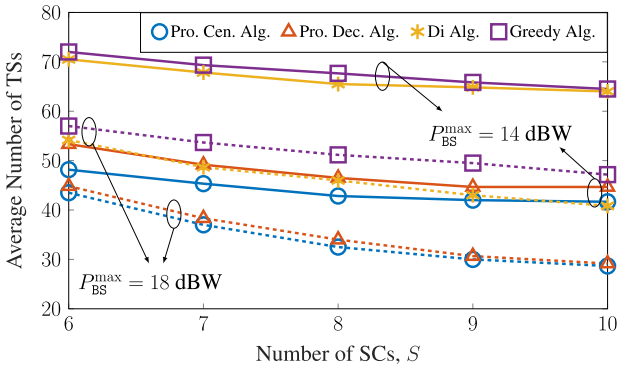

Fig. 11. The number of TSs versus the number of SCs.

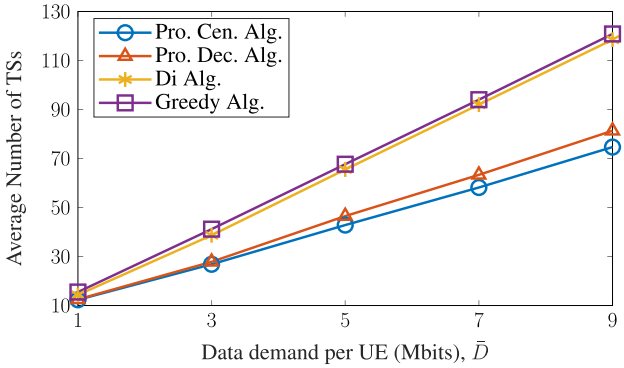

Fig. 12. Required-TS number vs. UE data demand.

Especially, when S varies from 8 to 10, the changes in the average number of TSs for the proposed *Cen-Alg* and *Dec-Alg*, the Di Algorithm, and the Greedy Algorithm are only about 1.2, 1.9, 1.5, and 3 TSs, respectively. Similar to the result shown in Fig. 10, this indicates the presence of a backhaul link bottleneck. When we increase $P_{\text{BS}}^{\max}$ to 18 dBW, as expected, the number of SCs has shown a more significant impact on the number of TSs. In this case, the Di Algorithm shows better transmission time performance compared to that of the Greedy Algorithm. However, the performance gap between these benchmarks and the two proposed algorithms remains notable. In particular, in the setting of 10 SCs available at the BSs, the Di Algorithm and the Greedy Algorithm require about 40.8 and 47.1 TSs, respectively, while the proposed algorithms require only about 28.6 and 29.1 TSs.

Additionally, Fig. 12 presents the TS numbers of four schemes as the functions of transmission data-amount demanding by each UE, $\bar{D}$. For all considered algorithms, the required TS numbers of all schemes appear to increase linearly as the data demand per UE escalates. Notably, the gaps between the proposed algorithms and the benchmarks are proportionally linear to $\bar{D}$. For instance, at $\bar{D} = 3$ Mbits, the required-TS gaps from the *Cen-Alg* and *Dec-Alg* to the Di Algorithm are about 11.8 and 11.2 TSs, respectively. Conversely, at $\bar{D} = 9$ Mbits, these gaps grow to about 43.9 and 37.2 TSs. Again, this figure confirms the effectiveness of the two proposed algorithms in comparison to the two benchmark algorithms when the data demand of the UE increases.

Fig. 13 illustrates the impact of variations in the number of UEs on transmission time performance. With fixed resources,

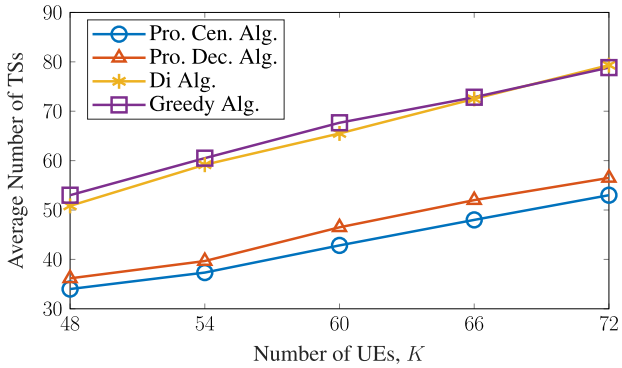

Fig. 13. Required-TS number vs. UE number.

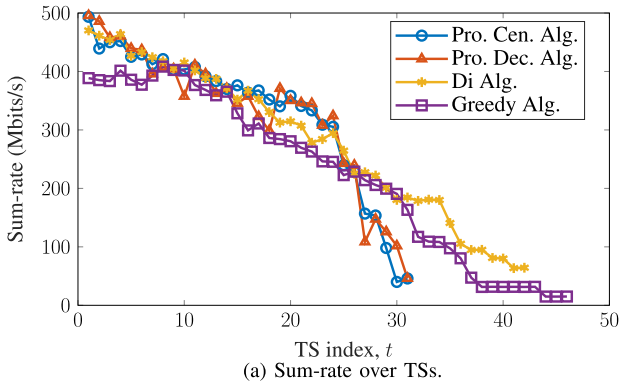

(a) Sum-rate over TSs.

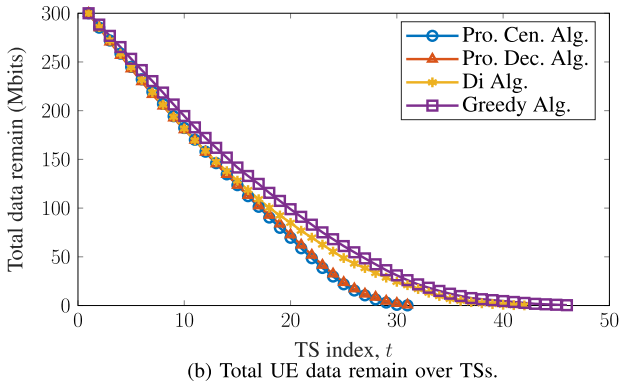

(b) Total UE data remain over TSs.

Fig. 14. Sum-rate system and data remain versus TS of a realization with $P_{\text{BS}}^{\max} = 18$ dBW.

it is observed that an increased number of UEs necessitates more TSs to meet the data demand for all UEs. As expected, the solutions provided by the two proposed algorithms surpass those of both the Di Algorithm and the Greedy Algorithm in terms of transmission time across all instances of K. Notably, the transmission time performance gaps between the two proposed algorithms and the two benchmark algorithms are significant and seem to remain relatively constant with different values of K, i.e., about 24 and 20 TSs from the *Cen-Alg* and *Dec-Alg* to the Di Algorithm, respectively. In addition to showcasing the superior performance of the two proposed algorithms in terms of minimizing transmission time, this figure also demonstrates the adaptability of our proposed algorithms with varying numbers of UEs in the network.

Next, Fig. 14a and 14b respectively present the achieved SR and total remaining UE data over TSs for the four considered algorithms for a particular realization. In almost all TS, Greedy

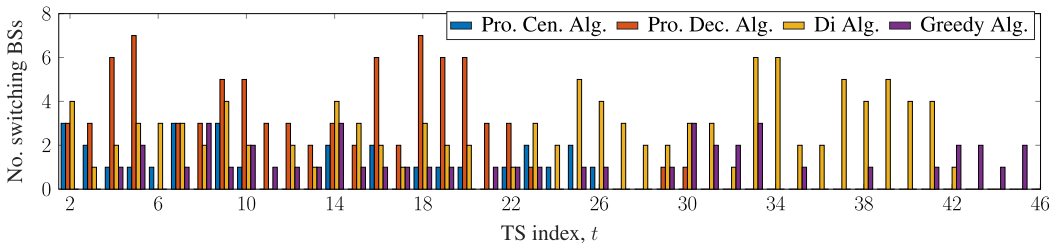

Fig. 15. The number of switching BSs over TSs.

Algorithm achieves the lowest SR performance, thus it requires the largest number of TSs to complete UE demand, i.e., 46 TSs. Regarding the other three algorithms, the differences among the SR achieved by these schemes are not significant, with similar totals of remaining data, in the duration from TS 1 to TS 15. In the subsequent TSs, the two proposed algorithms demonstrate superior SR performance; hence, they are able to fulfill UE data demand in fewer numbers of TSs compared to the benchmarks. Specifically, the outcomes of the proposed algorithms are 30 and 31 TSs, respectively, while the Di Algorithm requires 42 TSs. The reason for this phenomenon can be expressed as follows. After a certain TS, although the total remaining data for all algorithms is similar, the distribution of remaining data among UEs may differ. Therefore, adjusting the weight for the SR objective and accounting for capacity balancing in the two proposed algorithms can enhance SR performance. These figures further clarify the effectiveness of the two proposed algorithms.

Finally, Fig. 15 shows the number of BSs that have to switch their associated LEO over time. Herein, such BSs are so-called the switching BSs. As can be observed, the number of switching BSs due to Greedy Algorithm implementation is the lowest in almost all TSs due to the simple channel-gain-based BS-LEO association. While the proposed *Cen-Alg* returns the number of switching BSs lower than the other two remaining schemes, i.e., ranging from 1 to 3 BSs in nearly all TSs. Interestingly, the outcomes of the decentralized approach vary with large variance over the duration from TS 1 to TS 22 while Di Algorithm shows significant fluctuation in the following TSs. Additionally, the maximum number of switching BSs of these two algorithms are 7 and 6. Herein, the *Cen-Alg* has fewer switching BSs compared to the decentralized one but the returns of the latter are still acceptable, as the maximum number of HO BSs is 7 out of the total of 18 BSs. This can be interpreted as a trade-off between the two proposed algorithms in terms of workload offloading for the CNC.

C. Numerical-Result Discussion

1) The Superiority of Proposed Algorithms Compared to Benchmarks: In all considered scenarios, our two proposed algorithms demonstrate superior performance in terms of transmission time and achievable rates when compared to two baseline algorithms: the Greedy Algorithm and the Di Algorithm. The advantages of our proposed algorithms over these baselines are outlined as follows:

- Greedy Algorithm: establishing BS-UE and BS-LEOSat associations and SC assignments based solely on channel gain. The UE power allocation is performed using the water-filling algorithm, which does not account for interference, potentially leading to low performance.
- Di Algorithm: In this approach, UE transmit power is fixed. The resource management task is split into two separate problems for TN and NTN. As a result, this algorithm does not efficiently address interference management and two-tier user association issues.
- Our Proposed Algorithms: Our algorithms perform a comprehensive optimization of two-tier user associations, SC assignment, power control, and bandwidth allocation, all under the backhaul-link limitations. Moreover, by prioritizing users based on their remaining demand and incorporating UE fairness, our algorithms achieve a notable improvement in transmission time performance.

2) Comparable Performance of Decentralized and Centralized Algorithms: Both the *Cen-Alg* and *Dec-Alg* are developed using similar technical methods, resulting in the *Dec-Alg* having a performance comparable to that of the *Cen-Alg*. Specifically, in the decentralized approach, problem (27) from the centralized framework is divided into sub-problems $\mathcal{P}_{\mathsf{l},\mathsf{c}}^{\mathsf{clus}}$ for clusters as delineated in (37). Notably, each sub-problem $\mathcal{P}_{\mathsf{l},\mathsf{c}}^{\mathsf{clus}}$ shares a similar structure with (27). Consequently, we employ the same technical methods, namely compressed-sensing and SCALE methods, to solve them. The primary distinction between the centralized and decentralized solutions lies in the latter's requirement for updating the Lagrangian multiplier $\boldsymbol{\tau}$. This challenge is efficiently addressed using the sub-gradient descent method. Therefore, the *Dec-Alg* can obtain comparable performance to that of the *Cen-Alg*.

3) Practical Implementation Analysis: The studied network consists of two separate signal transmission hops, i.e., BS-UE and BS-LEOSat, which are processed on different frequency bands. Consequently, the synchronization procedures for these two hops can be conducted independently. For the BS-UE hop, we assume adherence to the 5G-NR standard. For the BS-LEOSat hop, the time and frequency synchronization can be conducted at each BS thanks to pre-compensation as outlined in the standard [30]. It is noted that both proposed algorithms are executed at the ground controllers without frequent signaling between LEOSats and ground segments. The eligible time consumption is the propagation time for channel estimation between BS and LEOSat. Hence, this time consumption is approximately 4 ms which is the round-trip-time between the LEOSat and the ground segment calculated based on the LEOSat altitude of 600 km.

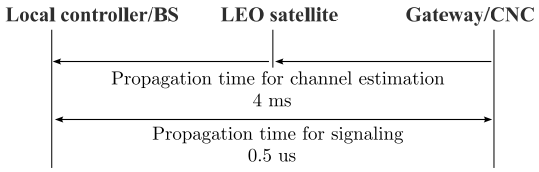

Fig. 16. Time consumption of propagation and signaling procedures.

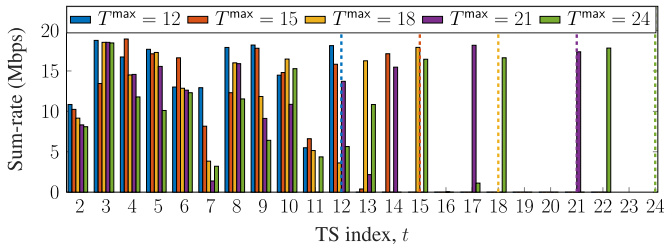

Fig. 17. Sum-rate of a delay-sensitive UE versus TS of a realization.

Next, as per the simulation settings of the simulation area and CNC location, the distance between CNC and LC is about 4.3 km, thus the transmission time between CNC and LC $T_{\mathsf{CNC,LC}} \leq 1.43 \times 10^{-8}$ s. On the other hand, it can be seen that the *Dec-Alg* requires about 15 Lagrangian iterations for convergence as per Fig. 7. Based on the data exchange procedure described in Fig. 4, the time consumption due to the signaling procedure can be calculated as $T_{\mathsf{sig}} \approx 0.5$ us. Summarily, the time consumption due to the propagation and data exchange is about 4.0005 ms, thus it is feasible to consider the TS duration of 30 ms. Therefore, this further demonstrates the practicality of the *Dec-Alg*. Specifically, the time consumption due to propagation and signaling procedure is described as per Fig. 16.

4) Impact of Temporary Link Disruption: Regarding one user's data transmission during a specific time window, temporary link disruptions can occur when no system resources are allocated for data transmission in one or multiple time slots (TSs). Such disruptions can cause latency and delays, which are particularly critical for users with stringent delay requirements, referred to as delay-sensitive UEs (DUEs). Let $\mathcal{K}_{\mathsf{sen}}$ be the DUE set. Regarding the delay requirements of the DUEs, we consider the following additional constraints,

$$(C_{\mathsf{DI}}):\ t_k \leq T_k^{\max},\ \forall k \in \mathcal{K}_{\mathsf{sen}},\ \text{and}\ d_k(t_k) = 0,\ \forall k, \tag{46}$$

wherein t_k indicates the TS in that the $\mathtt{DUE}_k$ can finish transmitting all data while $T_k^{\max}$ stands for the delay tolerance of $\mathtt{DUE}_k$. To satisfy this constraint, we proposed the weight update approach instead of (21) as

$$\omega_k[t] = T_k^{\max}/(\max(0, T_k^{\max} - t) + \epsilon) d_k[t],\ \forall k \in \mathcal{K}_{\mathsf{sen}}. \tag{47}$$

Based on this, the DUEs have higher priority for resource allocation at the TS closed to their TS tolerance, i.e., $T_k^{\max}$.

To evaluate the effectiveness of this updated approach in meeting the delay requirements for DUEs, we consider an additional simulation scenario in which 20% of all UEs are

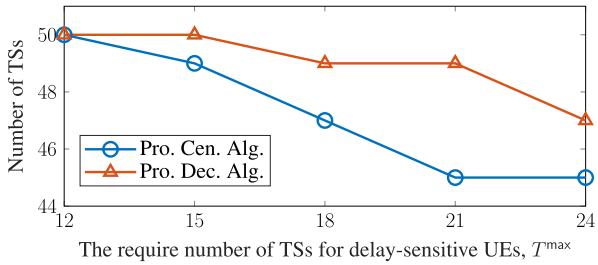

Fig. 18. Number of TSs versus T_{max} of a realization.

DUEs and their delay-tolerance for the DUEs varies from 12 to 24 TSs. In Fig. 17, one depicts the SR of a DUE with the different delay requirements $T_k^{\max}$, wherein the dashed lines indicate the delay requirements. It can be seen that the DUE transmits data continuously in almost all cases. Especially, the delay requirement is satisfied in all cases for this UE. However, the effort to satisfy the delay requirement impacts the overall system performance. Particularly, Fig. 18 shows the TS number to offload all UEs data for the various delay requirements $T_k^{\max}$. It can be observed that the required TS number increases due to the stricter delay requirements. This occurs because when higher priorities are set for the DUEs, the lower system resources are allocated to other users, leading to the degradation in overall system performance. This interestingly presents the trade-off between satisfying delay requirements and maintaining overall system performance.

VI. Conclusion

This work studied the novel joint two-tier association and RA for ISTNs over time regarding the mobility of satellites in the LEO constellation. An optimization problem focusing on minimizing transmission time under UE demand and backhaul link constraints was then considered. To address this problem, an iterative *Cen-Alg* implementable at the CNC is proposed. Moreover, with the objective of offloading computations from the central node, we proposed *Dec-Alg* capable of parallel execution at local network controllers efficiently. Through a range of numerical evaluations, both proposed algorithms demonstrated superior performance in terms of transmission time minimization and practicality, compared with two benchmarks. Additionally, the simulation results highlighted the proposed algorithms' effectiveness in terms of capacity balancing, SR performance, and adaptation ability, further validating their advantages and potential utility in real-world applications.

This study offers avenues for further extension, particularly in addressing the challenges of handover and scalability. Particularly, the handover between BSs and LEOSats, which consumes time for connection establishment and reduces system performance, should be minimized. These handovers need to be carefully considered in the optimization problem to avoid frequent occurrences. In terms of scalability, the controller link limitations at the CNC could lead to overload when scaling up the system. Therefore, scheduling for data exchange must be carefully planned for practical implementation. Additionally, the application of machine learning and

deep learning-based mechanisms offers promising prospects for enhancing user association and RA in ISTNs, especially utilizing learning-based techniques in the MINLP problems. These emerging techniques, as discussed in [54], [55] and [56], may facilitate comprehensive exploration in future research endeavors.

APPENDIX A
PROOF OF THEOREM 1

It can be easy to see that once $(C12)$ holds with equality, problems (26) and (27) are equivalent since the optimal solution of this problem is a feasible solution of the other and vice versa. For instance, let $(\mathbf{p}^*, \mathbf{P}^*, \mathbf{W}^*)$ be the optimal solution of problem (26). Then, denoting

$$\lambda^{\mathtt{UE}\prime}_{n,k}[t] = \sum_{\forall s\in\mathcal{S}} R^{\mathtt{UE},t}_{n,k,s}(\mathbf{p}^*[t]), \quad \forall (n,k)\in(\mathcal{N}\times\mathcal{K}), \tag{48a}$$

$$\lambda^{\mathtt{BS}\prime}_{n}[t] = \sum_{\forall m\in\mathcal{M}_t} R^{\mathtt{BS},t}_{m,n}(\mathbf{P}^*[t], \mathbf{W}^*[t]), \quad \forall n\in\mathcal{N}, \tag{48b}$$

yields $(\mathbf{p}^*, \mathbf{P}^*, \mathbf{W}^*, \boldsymbol{\lambda}^{\mathtt{UE}\prime}, \boldsymbol{\lambda}^{\mathtt{BS}\prime})$ as a feasible solution of (27). On another hand, one assume $(\mathbf{p}', \mathbf{P}', \mathbf{W}', \boldsymbol{\lambda}^{\mathtt{UE}\prime}, \boldsymbol{\lambda}^{\mathtt{BS}\prime})$ be the optimal solution of problem (27). Solving (28) to obtain $\mathbf{p}''$, we can easily prove that $\lambda^{\mathtt{UE}\prime}_{n,k}[t] = \sum_{\forall s\in\mathcal{S}} R^{\mathtt{UE},t}_{n,k,s}(\mathbf{p}''[t]), \forall(n,k)$. Interestingly, $(\mathbf{p}'', \mathbf{P}', \mathbf{W}', \boldsymbol{\lambda}^{\mathtt{UE}\prime}, \boldsymbol{\lambda}^{\mathtt{BS}\prime})$ is also an optimal solution of problem (27) since this set satisfies all constraints and returns the same objective as $(\mathbf{p}', \mathbf{P}', \mathbf{W}', \boldsymbol{\lambda}^{\mathtt{UE}\prime}, \boldsymbol{\lambda}^{\mathtt{BS}\prime})$. Furthermore, $(\mathbf{p}'', \mathbf{P}', \mathbf{W}')$ also satisfies all constraints of (26), and it should be a feasible solution of this problem.

APPENDIX B
PROOF OF PROPOSITION 1

This part provides the proof of Proposition 1, wherein SCALE method [43] is used to convexify $(C12)$. Specifically, at iteration i, the UE rate function can be lower bounded as

$$R^{\mathtt{UE},t}_{n,k,s}(\mathbf{p}[t]) \geq W_{\mathtt{SC}}(a^{(i)}_{n,k,s}[t]\ln(\mathtt{SINR}^{t}_{n,k,s}) + b^{(i)}_{n,k,s}[t]), \tag{49}$$

where the coefficients $a^{(i)}_{n,k,s}[t]$ and $b^{(i)}_{n,k,s}[t]$ are defined as

$$a^{(i)}_{n,k,s}[t] = \frac{\mathtt{SINR}^{t,(i-1)}_{n,k,s}}{1+\mathtt{SINR}^{t,(i-1)}_{n,k,s}}, b^{(i)}_{n,k,s}[t] = \log(1+\mathtt{SINR}^{t,(i-1)}_{n,k,s}) - a^{(i)}_{n,k,s}[t],$$

and $\mathtt{SINR}^{t,(i)}_{n,k,s} = \gamma^{\mathtt{UE},t}_{n,k,s}(\mathbf{p}^{(i)}[t])$ is the SINR value at iteration i.

Subsequently, to convexify the function $\ln(\mathtt{SINR}^{t}_{n,k,s})$ in (49), one introduces new variables $\{\bar{p}_{n,k,s}[t]\}$ and replace $p_{n,k,s}[t]$ with $p_{n,k,s}[t] = \exp(\bar{p}_{n,k,s}[t])$, $\forall(n,k,s)$. Based on that, (49) can be rewritten as

$$R^{\mathtt{UE},t}_{n,k,s}(\mathbf{p}[t]) \geq \tilde{R}^{\mathtt{UE},t}_{n,k,s}(\bar{\mathbf{p}}[t]) := W_{\mathtt{SC}}(a^{(i)}_{n,k,s}[t]\Psi^{t}_{n,k,s}(\bar{\mathbf{p}}[t]) + b^{(i)}_{n,k,s}[t]). \tag{50}$$

It is worth noting that the log-sum-exp term in $\Psi^{t}_{n,k,s}(\bar{\mathbf{p}}[t])$ is convex, thus $\tilde{R}^{\mathtt{UE},t}_{n,k,s}(\bar{\mathbf{p}}[t])$ is naturally concave. Exploiting this approach, constraint $(C12)$ can be approximated as $(\bar{C}12)$ in (50). In addition, regarding $\bar{p}_{n,k,s}[t]$, constraints $(\tilde{C}1)-(\tilde{C}3)$ and $(\tilde{C}7)$ are rewritten as $(\bar{C}1)-(\bar{C}3)$ and $(\bar{C}7)$ in (50) due to the transformation $p_{n,k,s}[t] = \exp(\bar{p}_{n,k,s}[t])$, respectively. It is worth noting that the replacing constraints $(\bar{C}1)-(\bar{C}3)$ and $(\bar{C}7)$ are convex thanks to the sum-exp forms.

APPENDIX C
PROOF OF PROPOSITION 4

Problem $(\mathcal{P}_{\mathsf{II}})$ formed by aggregating all cluster subproblems $(\mathcal{P}^{\mathsf{clus}}_{\mathsf{II},\mathsf{c}})$, $\forall c$, can be formulated as

$$(\mathcal{P}_{\mathsf{II}}) \quad \max_{\substack{\{\mathbf{p}_c,\mathbf{P}_c,\mathbf{W}_c,\\ \boldsymbol{\lambda}^{\mathtt{UE}}_c,\boldsymbol{\lambda}^{\mathtt{BS}}_c\}_{\forall c}}} \sum_{\forall c}\Big(\sum_{\substack{\forall n\in\mathcal{N}_c\\ \forall k\in\mathcal{K}_c}}\omega_k[t]\lambda^{\mathtt{UE}}_{n,k}[t] - \sum_{\forall m\in\mathcal{M}_t}\tau_m[t]\sum_{\forall n\in\mathcal{N}_c}W^{\mathtt{BS}}_{m,n}[t]\Big)$$
$$\text{s.t. } (\bar{C}1)_c - (\bar{C}3)_c, (\tilde{C}4)_c, (\bar{C}7)_c, (C8)_c, (C11)_c,$$
$$(C13)_c, (\bar{C}14)_c, \ \forall c.$$

By integrating the variables and index sets, the aggregation set of constraints $(\bar{C}1)_c - (\bar{C}3)_c, (\tilde{C}4)_c, (\bar{C}7)_c, (C8)_c, (C11)_c, (C13)_c, \forall c$ are equivalent to $(\bar{C}1)-(\bar{C}3), (\tilde{C}4), (\bar{C}7), (C8), (C11), (C13)$, respectively. In addition, if we suppose that the inter-cluster interference is very minimal $I^{c}_{n,s} \approx 0$, the approximated rate function $\Psi^{c,t}_{n,k,s}(\mathbf{p}_c[t]) = \Psi^{t}_{n,k,s}(\mathbf{p}[t])$. Hence, the aggregation set of constraints $(\bar{C}14)_c, \forall c$ is equivalent to constraint $(\bar{C}12)$. Subsequently, problem $(\mathcal{P}_{\mathsf{II}})$ can be rewritten as

$$(\mathcal{P}_{\mathsf{II}}) \quad \max_{\mathbf{p},\mathbf{P},\mathbf{W},\boldsymbol{\lambda}^{\mathtt{UE}},\boldsymbol{\lambda}^{\mathtt{BS}}} \sum_{\forall(n,k)}\omega_k[t]\lambda^{\mathtt{UE}}_{n,k}[t] + \sum_{\forall m\in\mathcal{M}_t}\tau_m[t](W^{\mathtt{LEO}}_{m} - \sum_{\forall n\in\mathcal{N}}W^{\mathtt{BS}}_{m,n}[t])$$
$$\text{s.t. } (\bar{C}1)-(\bar{C}3), (\tilde{C}4), (\bar{C}7), (C8),$$
$$(C11), (\bar{C}12), (C13),$$

wherein the term $\sum_{\forall m}\tau_m[t]W^{\mathtt{LEO}}_{m}$ is added to the objective to restore the relaxed form of BW constraint associated with $\boldsymbol{\tau}$, that does not change the optimality of problem $(\mathcal{P}_{\mathsf{II}})$.

Let denote $\mathcal{F}_{\mathsf{II}} \triangleq \{\Omega | \Omega \text{ satisfies } (\bar{C}1)-(\bar{C}3), (\tilde{C}4), (\bar{C}7), (C8), (C11), (\bar{C}12), (C13)\}$ is the feasible set of the relaxed problem $(\mathcal{P}_{\mathsf{II}})$, the dual problem of $(\mathcal{P}_{\mathsf{II}})$ can be expressed as

$$(\mathcal{D}_{\mathsf{II}}) \ \min_{\boldsymbol{\tau}} \ \sup_{\Omega\in\mathcal{F}_{\mathsf{II}}} L(\Omega,\boldsymbol{\tau}) \text{ s.t. } \tau_m[t]\geq 0, \ \forall(m,t), \tag{51}$$

where $L(\Omega,\boldsymbol{\tau}) = \sum_{\forall(n,k)}\omega_k[t]\lambda^{\mathtt{UE}}_{n,k}[t] + \sum_{\forall m\in\mathcal{M}_t}\tau_m[t](W^{\mathtt{LEO}}_{m} - \sum_{\forall n\in\mathcal{N}}W^{\mathtt{BS}}_{m,n}[t])$. Notably, problem $(\mathcal{D}_{\mathsf{II}})$ is also the dual problem of (29). Since the problem (29) is convex, the strong duality holds for $(\mathcal{D}_{\mathsf{II}})$ and (29).

ACKNOWLEDGMENT

For the purpose of open access, and in fulfillment of the obligations arising from the grant agreement, the author has applied a Creative Commons Attribution 4.0 International (CC BY 4.0) license to any Author Accepted Manuscript version arising from this submission.

REFERENCES

[1] H. Nguyen-Kha, V. N. Ha, E. Lagunas, S. Chatzinotas, and J. Grotz, "Two-tier user association and resource allocation design for integrated satellite-terrestrial networks," in *Proc. IEEE Int. Conf. Commun. Workshops (ICC Workshops)*, May 2023, pp. 1234–1239.

[2] C.-X. Wang et al., "On the road to 6G: Visions, requirements, key technologies, and testbeds," *IEEE Commun. Surveys Tuts.*, vol. 25, no. 2, pp. 905–974, 2nd Quart. 2023.

[3] H. Tataria, M. Shafi, A. F. Molisch, M. Dohler, H. Sjöland, and F. Tufvesson, "6G wireless systems: Vision, requirements, challenges, insights, and opportunities," *Proc. IEEE*, vol. 109, no. 7, pp. 1166–1199, Jul. 2021.

[4] M. Giordani, M. Polese, M. Mezzavilla, S. Rangan, and M. Zorzi, "Toward 6G networks: Use cases and technologies," *IEEE Commun. Mag.*, vol. 58, no. 3, pp. 55–61, Mar. 2020.

[5] V. N. Ha, E. Lagunas, T. S. Abdu, H. Chaker, S. Chatzinotas, and J. Grotz, "Large-scale beam placement and resource allocation design for MEO-constellation SATCOM," in *Proc. IEEE Int. Conf. Commun. Workshops (ICC Workshops)*, May 2023, pp. 1240–1245.

[6] T. S. Abdu, E. Lagunas, V. N. Ha, J. Grotz, S. Kisseleff, and S. Chatzinotas, "Demand-aware flexible handover strategy for LEO constellation," in *Proc. IEEE Int. Conf. Commun. Workshops (ICC Workshops)*, May 2023, pp. 978–983.

[7] C. Handforth, H. Croxson, and G. Cruz, "Closing the coverage gap: How innovation can drive rural connectivity," GSMA, London, U.K., 2019. [Online]. Available: https://www.gsma.com/solutions-and-impact/connectivity-for-good/mobile-for-development/gsma_resources/closing-the-coverage-gap-how-innovation-can-drive-rural-connectivity/

[8] X. Zhu and C. Jiang, "Integrated satellite-terrestrial networks toward 6G: Architectures, applications, and challenges," *IEEE Internet Things J.*, vol. 9, no. 1, pp. 437–461, Jan. 2022.

[9] B. Tezergil and E. Onur, "Wireless backhaul in 5G and beyond: Issues, challenges and opportunities," *IEEE Commun. Surveys Tuts.*, vol. 24, no. 4, pp. 2579–2632, 4th Quart., 2022.

[10] O. Kodheli et al., "Satellite communications in the new space era: A survey and future challenges," *IEEE Commun. Surveys Tuts.*, vol. 23, no. 1, pp. 70–109, 1st Quart., 2021.

[11] H. Nguyen-Kha, V. N. Ha, E. Lagunas, S. Chatzinotas, and J. Grotz, "LEO-to-user assignment and resource allocation for uplink transmit power minimization," in *Proc. WSA SCC 26th Int. ITG Workshop Smart Antennas 13th Conf. Syst., Commun., Coding*, Feb. 2023, pp. 1–6.

[12] X. Lin, S. Cioni, G. Charbit, N. Chuberre, S. Hellsten, and J.-F. Boutillon, "On the path to 6G: Embracing the next wave of low Earth orbit satellite access," *IEEE Commun. Mag.*, vol. 59, no. 12, pp. 36–42, Dec. 2021.

[13] G. Geraci, D. López-Pérez, M. Benzaghta, and S. Chatzinotas, "Integrating terrestrial and non-terrestrial networks: 3D opportunities and challenges," *IEEE Commun. Mag.*, vol. 61, no. 4, pp. 42–48, Apr. 2023.

[14] N. U. Hassan, C. Huang, C. Yuen, A. Ahmad, and Y. Zhang, "Dense small satellite networks for modern terrestrial communication systems: Benefits, infrastructure, and technologies," *IEEE Wireless Commun.*, vol. 27, no. 5, pp. 96–103, Oct. 2020.

[15] J. Du, C. Jiang, A. Benslimane, S. Guo, and Y. Ren, "SDN-based resource allocation in edge and cloud computing systems: An evolutionary Stackelberg differential game approach," *IEEE/ACM Trans. Netw.*, vol. 30, no. 4, pp. 1613–1628, Aug. 2022.

[16] J. Li, K. Xue, D. S. L. Wei, J. Liu, and Y. Zhang, "Energy efficiency and traffic offloading optimization in integrated satellite/terrestrial radio access networks," *IEEE Trans. Wireless Commun.*, vol. 19, no. 4, pp. 2367–2381, Apr. 2020.

[17] S. Chan, H. Lee, S. Kim, and D. Oh, "Intelligent low complexity resource allocation method for integrated satellite-terrestrial systems," *IEEE Wireless Commun. Lett.*, vol. 11, no. 5, pp. 1087–1091, May 2022.

[18] Z. Gao, A. Liu, C. Han, and X. Liang, "Max completion time optimization for Internet of Things in LEO satellite-terrestrial integrated networks," *IEEE Internet Things J.*, vol. 8, no. 12, pp. 9981–9994, Jun. 2021.

[19] L. Zhang, H. Zhang, C. Guo, H. Xu, L. Song, and Z. Han, "Satellite-aerial integrated computing in disasters: User association and offloading decision," in *Proc. IEEE Conf. Commun.*, Jul. 2020, pp. 554–559.

[20] Y. Zhang, H. Zhang, H. Zhou, and W. Li, "Interference cooperation based resource allocation in NOMA terrestrial-satellite networks," in *Proc. IEEE Global Commun. Conf. (GLOBECOM)*, Dec. 2021, pp. 1–5.

[21] B. Di, H. Zhang, L. Song, Y. Li, and G. Y. Li, "Ultra-dense LEO: Integrating terrestrial-satellite networks into 5G and beyond for data offloading," *IEEE Trans. Wireless Commun.*, vol. 18, no. 1, pp. 47–62, Jan. 2019.

[22] R. Deng, B. Di, S. Chen, S. Sun, and L. Song, "Ultra-dense LEO satellite offloading for terrestrial networks: How much to pay the satellite operator?" *IEEE Trans. Wireless Commun.*, vol. 19, no. 10, pp. 6240–6254, Oct. 2020.

[23] R. Deng, B. Di, H. Zhang, and L. Song, "Ultra-dense LEO satellite constellation design for global coverage in terrestrial-satellite networks," in *Proc. GLOBECOM IEEE Global Commun. Conf.*, Dec. 2020, pp. 1–6.

[24] R. Deng, B. Di, H. Zhang, L. Kuang, and L. Song, "Ultra-dense LEO satellite constellations: How many LEO satellites do we need?" *IEEE Trans. Wireless Commun.*, vol. 20, no. 8, pp. 4843–4857, Aug. 2021.

[25] C.-Q. Dai, J. Luo, S. Fu, J. Wu, and Q. Chen, "Dynamic user association for resilient backhauling in satellite–terrestrial integrated networks," *IEEE Syst. J.*, vol. 14, no. 4, pp. 5025–5036, Dec. 2020.

[26] R. M. Calvo et al., "Optical feeder links for future very high-throughput satellite systems in B5G networks," in *Proc. Eur. Conf. Opt. Commun. (ECOC)*, Dec. 2020, pp. 1–4.

[27] Z. Xiao et al., "LEO satellite access network (LEO-SAN) towards 6G: Challenges and approaches," *IEEE Wireless Commun.*, vol. 31, no. 2, pp. 89–96, Apr. 2024.

[28] *Study on New Radio (NR) to Support Non-Terrestrial Networks*, Standard Technical report (TR) 38.811, Version 15.4.0, 3GPP, Sep. 2020.

[29] *Study on Satellite Access Phase 3*, Standard Technical report (TR) 22.865, 3GPP, Version 19.0.0, Jun. 2023.

[30] *Solutions for NR to Support Non-Terrestrial Networks*, Standard Technical Report (TR) 38.821, Version 16.2.0, 3GPP, Mar. 2023.

[31] C. Caini, H. Cruickshank, S. Farrell, and M. Marchese, "Delay- and disruption-tolerant networking (DTN): An alternative solution for future satellite networking applications," *Proc. IEEE*, vol. 99, no. 11, pp. 1980–1997, Nov. 2011.

[32] L. You et al., "Hybrid analog/digital precoding for downlink massive MIMO LEO satellite communications," *IEEE Trans. Wireless Commun.*, vol. 21, no. 8, pp. 5962–5976, Aug. 2022.

[33] V. N. Ha, T. T. Nguyen, E. Lagunas, J. C. Merlano Duncan, and S. Chatzinotas, "GEO payload power minimization: Joint precoding and beam hopping design," in *Proc. IEEE Global Commun. Conf. (GLOBECOM)*, Rio de Janeiro, Brazil, Jun. 2022, pp. 6445–6450.

[34] A. Alimohammad, "Compact Rayleigh and Rician fading simulator based on random walk processes," *IET Commun.*, vol. 3, pp. 1333–1342, Aug. 2009.

[35] S. Haggui, F. Rouissi, Y. Mlayeh, and F. Tlili, "A compact architecture of a mobile-to-mobile fading channel emulator based on random walk process," in *Proc. 5th Int. Conf. Multimedia Comput. Syst. (ICMCS)*, Sep. 2016, pp. 564–569.

[36] V. N. Ha, T. T. Nguyen, L. B. Le, and J.-F. Frigon, "Admission control and network slicing for multi-numerology 5G wireless networks," *IEEE Netw. Lett.*, vol. 2, no. 1, pp. 5–9, Mar. 2020.

[37] T. T. Nguyen, V. N. Ha, and L. B. Le, "Wireless scheduling for heterogeneous services with mixed numerology in 5G wireless networks," *IEEE Commun. Lett.*, vol. 24, no. 2, pp. 410–413, Feb. 2020.

[38] J. Du, C. Jiang, H. Zhang, Y. Ren, and M. Guizani, "Auction design and analysis for SDN-based traffic offloading in hybrid satellite-terrestrial networks," *IEEE J. Sel. Areas Commun.*, vol. 36, no. 10, pp. 2202–2217, Oct. 2018.

[39] F. She, H. Luo, W. Chen, and X. Wang, "Joint queue control and user scheduling in MIMO broadcast channel under zero-forcing multiplexing," in *Proc. IEEE Int. Conf. Commun.*, May 2008, pp. 275–279.

[40] H. Viswanathan and K. Kumaran, "Rate scheduling in multiple antenna downlink wireless systems," *IEEE Trans. Commun.*, vol. 53, no. 4, pp. 645–655, Apr. 2005.

[41] E. Candes, M. Wakin, and S. Boyd, "Enhancing sparsity by reweighted L1 minimization," *J. Fourier Anal. Appl.*, vol. 14, pp. 877–905, Dec. 2008.

[42] V. N. Ha, L. B. Le, and N.-D. Dao, "Coordinated multipoint transmission design for cloud-RANs with limited fronthaul capacity constraints," *IEEE Trans. Veh. Technol.*, vol. 65, no. 9, pp. 7432–7447, Sep. 2016.

[43] J. Papandriopoulos and J. Evans, "Low-complexity distributed algorithms for spectrum balancing in multi-user DSL networks," in *Proc. IEEE Int. Conf. Commun.*, Jun. 2006, pp. 3270–3275.

[44] M. Monteiro, N. Lindqvist, and A. Klautau, "Spectrum balancing algorithms for power minimization in DSL networks," in *Proc. IEEE Int. Conf. Commun.*, Jun. 2009, pp. 1–5.

[45] J. Li, L. Zhang, K. Xue, Y. Fang, and Q. Sun, "Secure transmission by leveraging multiple intelligent reflecting surfaces in MISO systems," *IEEE Trans. Mobile Comput.*, vol. 22, no. 4, pp. 2387–2401, Apr. 2023.

[46] S. Boyd and J. Park, "Subgradient methods," Spring Quarter, Stanford Univ., Stanford, CA, USA, App. note Lect. Notes EE364b, 2014.

[47] S. P. Boyd and L. Vandenberghe, *Convex Optimization*. Cambridge, U.K.: Cambridge Univ. Press, 2004.

[48] J. Dahl and E. D. Andersen, "A primal-dual interior-point algorithm for nonsymmetric exponential-cone optimization," *Math. Program.*, vol. 194, nos. 1–2, pp. 341–370, Jul. 2022.

[49] A. Serrano, "Algorithms for unsymmetric cone optimization and an implementation for problems with the exponential cone," M.S. thesis, Inst. Comput. Math. Eng., Stanford Univ., Stanford, CA, USA, 2015. [Online]. Available: http://purl.stanford.edu/sn367tt9726

[50] A. Skajaa and Y. Ye, "A homogeneous interior-point algorithm for nonsymmetric convex conic optimization," *Math. Program.*, vol. 150, no. 2, pp. 391–422, May 2015.
[51] G. Zheng, S. Chatzinotas, and B. Ottersten, "Generic optimization of linear precoding in multibeam satellite systems," *IEEE Trans. Wireless Commun.*, vol. 11, no. 6, pp. 2308–2320, Jun. 2012.
[52] E. Salonen and S. Uppala, "New prediction method of cloud attenuation," *Electron. Lett.*, vol. 27, no. 12, p. 1106, 1991, doi: 10.1049/el:19910687.
[53] I. Ali, N. Al-Dhahir, and J. E. Hershey, "Doppler characterization for LEO satellites," *IEEE Trans. Commun.*, vol. 46, no. 3, pp. 309–313, Mar. 1998.
[54] J. Du, C. Jiang, J. Wang, Y. Ren, and M. Debbah, "Machine learning for 6G wireless networks: Carrying forward enhanced bandwidth, massive access, and ultrareliable/low-latency service," *IEEE Veh. Technol. Mag.*, vol. 15, no. 4, pp. 122–134, Dec. 2020.
[55] T. M. Kebedew, V. N. Ha, E. Lagunas, D. D. Tran, J. Grotz, and S. Chatzinotas, "Reinforcement learning for QoE-oriented flexible bandwidth allocation in satellite communication networks," in *Proc. IEEE Globecom Workshops (GC Wkshps)*, Dec. 2023, pp. 305–310.
[56] G. Fontanesi, "Artificial intelligence for satellite communication and non-terrestrial networks: A survey," 2023, *arXiv:2304.13008*.

Hung Nguyen-Kha (Graduate Student Member, IEEE) received the B.E. degree in electronic and telecommunication from the Posts and Telecommunications Institute of Technology, Hanoi, Vietnam, in 2019, and the M.S. degree in electrical engineering from Soongsil University, South Korea, in 2021. From 2019 to 2021, he was with the Wireless Communication Laboratory, Soongsil University. Since 2022, he has been a Doctoral Researcher with the Interdisciplinary Centre for Security, Reliability and Trust (SnT), University of Luxembourg. His research interests include applied optimization and machine-learning techniques for RRM problems in wireless communication systems, including SatCom, 5G/beyond-5G, and massive MIMO.

Vu Nguyen Ha (Senior Member, IEEE) received the B.Eng. degree (Hons.) from French Training Program for Excellent Engineers in Vietnam, Ho Chi Minh City University of Technology, Vietnam, the Addendum degree from the Groupe des École des Télécommunications, École Nationale Supérieure des Télécommunications de Bretagne, Bretagne, France, in 2007, and the Ph.D. degree (Hons.) from the Institut National de la Recherche Scientifique-Énergie, Matériaux et Télécommunications, Université du Québec, Montreal, QC, Canada, in 2017. From 2016 to 2021, he was a Post-Doctoral Fellow with École Polytechnique de Montreal and then the Resilient Machine Learning Institute, École de Technologie Supérieure, University of Quebec. He is currently a Research Scientist with the Interdisciplinary Centre for Security, Reliability, and Trust, University of Luxembourg. His research interests include applying/developing optimization and machine-learning-based solutions for RRM problems in MAC/PHY layers of several wireless communication systems, including SATCOM, 5G/beyond-5G, HetNets, Cloud RAN, massive MIMO, mobile edge computing, and 802.11ax WiFi. He received the Innovation Award for the Ph.D. degree. He was a recipient of the FRQNT Postdoctoral Fellowship for International Researcher (PBEEE) awarded by Quebec Ministry of Education, Canada, in 2018 and 2019. In 2021 and 2022, he received the Certificate for Exemplary Reviews by IEEE WIRELESS COMMUNICATIONS LETTERS.

Eva Lagunas (Senior Member, IEEE) received the M.Sc. and Ph.D. degrees in telecommunications engineering from the Polytechnic University of Catalonia (UPC), Barcelona, Spain, in 2010 and 2014, respectively. She has held positions at UPC; the Centre Tecnologic de Telecomunicacions de Catalunya (CTTC), University of Pisa, Italy; and the Center for Advanced Communications (CAC), Villanova University, PA, USA. In 2014, she joined the Interdisciplinary Centre for Security, Reliability and Trust (SnT), University of Luxembourg, where she is currently a Research Scientist. Her research interests include terrestrial and satellite system optimization, spectrum sharing, resource management, and machine learning.

Symeon Chatzinotas (Fellow, IEEE) received the M.Eng. degree in telecommunications from the Aristotle University of Thessaloniki, Greece, in 2003, and the M.Sc. and Ph.D. degrees in electronic engineering from the University of Surrey, U.K., in 2006 and 2009, respectively. He is currently a Full Professor/the Chief Scientist I and the Head of the Research Group SIGCOM, Interdisciplinary Centre for Security, Reliability and Trust, University of Luxembourg. He is also an Adjunct Professor with the Department of Electronic Systems, Norwegian University of Science and Technology, and a Collaborating Scholar with the Institute of Informatics and Telecommunications, National Center for Scientific Research "Demokritos." In the past, he was a Visiting Professor with the University of Parma, Italy, and contributed in numerous research and development projects for the Institute of Telematics and Informatics, Center of Research and Technology Hellas, and the Mobile Communications Research Group, Center of Communication Systems Research, University of Surrey. He has authored more than 700 technical papers in refereed international journals, conferences, and scientific books. He has received numerous awards and recognitions, including the IEEE Fellowship and an IEEE Distinguished Contributions Award. He is on the editorial board of IEEE TRANSACTIONS ON COMMUNICATIONS, IEEE OPEN JOURNAL OF VEHICULAR TECHNOLOGY, and *International Journal of Satellite Communications and Networking*.

Joel Grotz (Senior Member, IEEE) received the joint degree in electrical engineering from the University of Karlsruhe and the Grenoble Institute of Technology in 1999 and the joint Ph.D. degree in telecommunications jointly from the University of Luxembourg and KTH, Stockholm, in 2008. He was with SES, Betzdorf, Luxembourg, on the development of satellite broadband communication system design for GEO and MEO high-throughput satellite systems on different ground segment and space segment topics and system optimization aspects. He was with the Technical Laboratories, ST Engineering iDirect (former Newtec Cy with Sint-Niklaas in Belgium) on topics of system design and signal processing in satellite modems. He is currently a Senior Manager with SES on the development of a dynamic resource management system for novel flexible satellite systems, including SES-17 and O3b mPOWER and future satellite systems under planning.